


Peripheral Inflammation, Apolipoprotein E4, and Amyloid- β Interact to Induce Cognitive and Cerebrovascular Dysfunction

Felecia M. Marottoli¹, Yuriko Katsumata², Kevin P. Koster¹,
Riya Thomas¹, David W. Fardo^{2,3}, and Leon M. Tai¹

ASN Neuro
July-August 2017: 1–19
© The Author(s) 2017
Reprints and permissions:
sagepub.co.uk/journalsPermissions.nav
DOI: 10.1177/1759091417719201
journals.sagepub.com/home/asn


Abstract

Cerebrovascular dysfunction is rapidly reemerging as a major process of Alzheimer's disease (AD). It is, therefore, crucial to delineate the roles of AD risk factors in cerebrovascular dysfunction. While *apolipoprotein E4* (*APOE4*), Amyloid- β ($A\beta$), and peripheral inflammation independently induce cerebrovascular damage, their collective effects remain to be elucidated. The goal of this study was to determine the interactive effect of *APOE4*, $A\beta$, and chronic repeated peripheral inflammation on cerebrovascular and cognitive dysfunction *in vivo*. EFAD mice are a well-characterized mouse model that express human *APOE3* (E3FAD) or *APOE4* (E4FAD) and overproduce human $A\beta_{42}$ via expression of 5 Familial Alzheimer's disease (5xFAD) mutations. Here, we utilized EFAD carriers [5xFAD^{+/-}/*APOE*^{+/-} (EFAD+)] and noncarriers [5xFAD^{-/-}/*APOE*^{+/-} (EFAD-)] to compare the effects of peripheral inflammation in the presence or absence of human $A\beta$ overproduction. Low-level, chronic repeated peripheral inflammation was induced in EFAD mice via systemic administration of lipopolysaccharide (LPS; 0.5 mg/kg/wk i.p.) from 4 to 6 months of age. In E4FAD+ mice, peripheral inflammation caused cognitive deficits and lowered post-synaptic protein levels. Importantly, cerebrovascular deficits were observed in LPS-challenged E4FAD+ mice, including cerebrovascular leakiness, lower vessel coverage, and cerebral amyloid angiopathy-like $A\beta$ deposition. Thus, *APOE4*, $A\beta$, and peripheral inflammation interact to induce cerebrovascular damage and cognitive deficits.

Keywords

inflammation, Alzheimer's disease, apolipoprotein E4, cerebrovasculature

Received March 9, 2017; Received revised May 30, 2017; Accepted for publication June 7, 2017

Introduction

Cerebrovascular dysfunction is resurfacing as a critical pathological component of the onset and progression of cognitive decline in Alzheimer's disease (AD; Love and Miners, 2016). Indeed, vascular risk factors that are linked to cerebrovascular dysfunction increase AD risk and progression (Farkas and Luiten, 2001; Iadecola, 2004; Henry-Feugeas, 2008; de la Torre, 2010; Zlokovic, 2011; Stanimirovic and Friedman, 2012; van de Haar et al., 2015). Further, increased cerebrovascular leakiness, reduced cerebral blood flow, and altered cerebrovascular coverage have all been demonstrated both in AD patients and mouse models of AD-like pathology (Ujii et al., 2003; Dickstein et al., 2006; Paul et al., 2007). Known AD risk factors and processes (which we

collectively term AD hits) may contribute to AD by disrupting the cerebrovasculature (Tai et al., 2016). As the homeostatic interface between the blood and the brain, the cerebrovasculature is susceptible to damage from AD hit-modulated processes from both the brain and

¹Department of Anatomy and Cell Biology, University of Illinois at Chicago, IL, USA

²Department of Biostatistics, University of Kentucky, Lexington, KY, USA

³Sanders-Brown Center on Aging, University of Kentucky, Lexington, KY, USA

Corresponding Author:

Leon M. Tai, University of Illinois at Chicago, Chicago, IL, USA.
Email: leontai@uic.edu



periphery. Therefore, dissecting the impact of AD hits on cerebrovascular dysfunction in AD is crucial.

Amyloid- β ($A\beta$), *apolipoprotein E4* (*APOE4*), and peripheral inflammation are key AD hits that are independently linked to AD progression and cerebrovascular dysfunction. High soluble and extracellular $A\beta$ levels are important features of AD. Furthermore, $A\beta$ disrupts brain endothelial cells *in vitro* (Koster et al., 2016) and mouse models that overproduce $A\beta$ via familial AD mutations are associated with cerebrovascular dysfunction (Giannoni et al., 2016). *APOE4* is the strongest genetic risk factor for AD and carries a 12-fold increase in risk compared to *APOE3* (Corder et al., 1993; Farrer et al., 1997; Bertram and Tanzi, 2004; Genin et al., 2011; Leoni, 2011). *APOE4* is also associated with increased cerebrovascular leakiness and lower capillary coverage in both aging and AD (reviewed in Tai et al., 2016). Chronic peripheral inflammation is a common feature of nongenetic peripheral AD risk factors. Type 2 diabetes, midlife hypercholesterolemia, midlife hypertension, and atherosclerosis all have a peripheral inflammatory component (Scalia et al., 1998; Duncan et al., 2003; Hansson et al., 2006; Savoia and Schiffrin, 2006). Acute peripheral inflammation also induces cerebrovascular damage *in vivo*, and cytokines disrupt brain endothelial cells *in vitro* (Aslam et al., 2012; Roberts et al., 2012; Lopez-Ramirez et al., 2013; Duperray et al., 2015; Qin et al., 2015). While $A\beta$, *APOE4*, and peripheral inflammation are independently associated with cerebrovascular dysfunction, increasing evidence for other AD-like pathology supports that they interact. For example, *APOE4* and peripheral risk factors interact to increase AD risk (Haan et al., 1999; Irie et al., 2008; Matsuzaki et al., 2010), *APOE4* is associated with higher $A\beta$ levels, and peripheral inflammation induces more severe hyperthermia with *APOE4* in humans (Gale et al., 2014). The goal of this study was to determine whether *in vivo*, *APOE4* and $A\beta$ predispose the cerebrovasculature to damage in response to chronic repeated peripheral inflammation.

EFAD mice (Youmans et al., 2012a; Tai et al., 2017) are a well-characterized mouse model that express human *APOE3* (E3FAD) or *APOE4* (E4FAD) and overproduce human $A\beta_{42}$ (EFAD+), whereas littermate controls express *APOE3* or *APOE4* in the absence of human $A\beta$ (EFAD-). Thus, EFAD mice are well-suited to determine the *APOE*-modulated contribution of AD relevant hits in the presence or absence of human $A\beta$. We therefore utilized EFAD mice in this study. Chronic repeated peripheral challenge with lipopolysaccharide (LPS; 0.5 mg/kg/wk, from 4 to 6 months of age) induced cognitive and cerebrovascular deficits in E4FAD+ mice. These data support that cerebrovascular dysfunction is a key mechanism that links AD hits to pathogenesis.

Materials and Methods

Animals

Breeding and colony maintenance was conducted at the University of Illinois at Chicago as previously described (Youmans et al., 2012a; Thomas et al., 2016), and all protocols adhere to the University of Illinois at Chicago Institutional Animal Care and Use Committee protocols.

EFAD mice express human *APOE3* or *APOE4* and overproduce human $A\beta$ via the expression of five Familial Alzheimer's disease (5xFAD) mutations (Youmans et al., 2012a). EFAD mice were generated by crossing *APOE*-targeted replacement (*APOE*-TR) mice on a C57/BL6 background with female 5xFAD mice on a C57BL6/B6xSJL background. The resulting male offspring were then backcrossed to female *APOE*-TR mice to produce 5xFAD^{+/-}/*APOE*^{+/+} (EFAD) mice. EFAD mice are maintained as an inbred strain, by crossing male EFAD+ with female EFAD- mice, or vice versa. Therefore, the offspring produced express human apoE as either carriers or noncarriers of the 5xFAD mutations (Youmans et al., 2012a).

Male EFAD carrier [5xFAD^{+/-}/*APOE*^{+/+} (EFAD+)] and noncarrier [5xFAD^{-/-}/*APOE*^{+/+} (EFAD-)] mice utilized in this study were grouped into 10 cohorts ($n \geq 8$ per cohort), and treatments were randomized by cage. Female mice were excluded from this study as female sex is in itself a risk factor for AD. We have previously demonstrated cognitive and cerebrovascular deficits in female E4FAD+ mice (Thomas et al., 2016). Therefore, the focus here was whether peripheral inflammation induces similar cerebrovascular and cognitive dysfunction in male E4FAD+ mice. EFAD mice used to begin the breeding colonies were a generous gift of Dr. M. J. LaDu. All investigators were blinded for LPS treatment.

LPS Treatment

EFAD mice were administered phosphate-buffered saline (PBS) or LPS (*Escherichia coli* O8:K27 [S-form], Innaxon) via intraperitoneal (i.p.) injection (0.5 mg/kg/wk) from 4 to 6 months of age. A final LPS treatment was administered the day before sacrifice for nine total injections (Figure 1(a)). Body weights were measured prior to each injection.

Behavioral Analysis

Behavioral tests to assess cognitive function were initiated 2 days after the eighth regular treatment injection of LPS or PBS and concluded 2 days prior to the final injection (Figure 1(a)). Mice were sequentially assessed (24 hr between tests) by spontaneous alternation (Y-maze) and novel object recognition tests as described in Thomas et al. (2016) with slight modification. All behavioral analysis

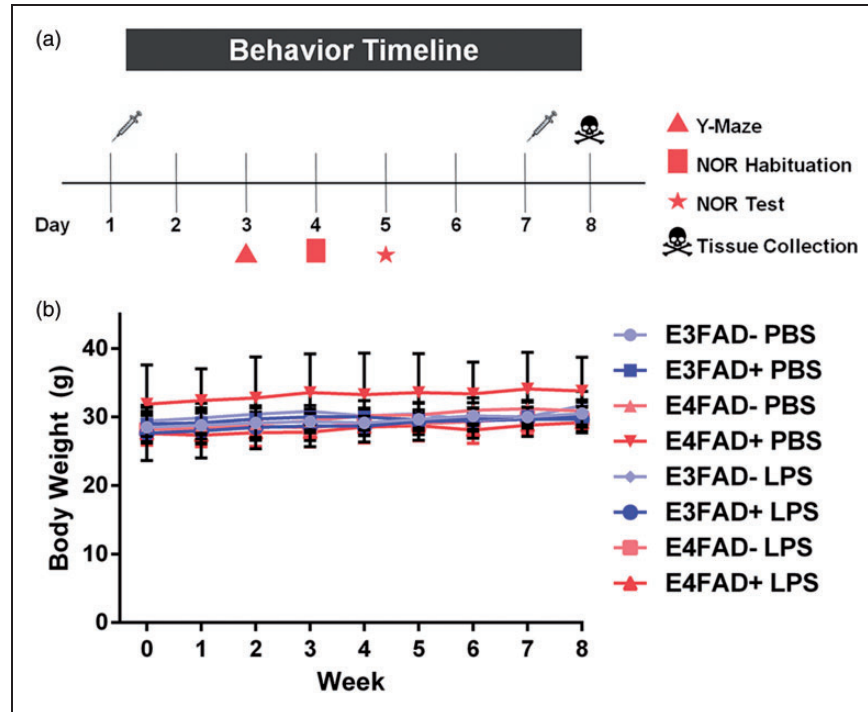


Figure 1. (a) Study design. (b) Body weight is unaffected by LPS treatment. Body weight was tracked weekly over the course of LPS treatment from 4 to 6 months of age. No differences were detected between genotypes or treatment groups. $p > .05$ using a mixed effects model.

was conducted during the mouse dark cycle, recorded by an overhead camera, and analyzed using ANY-Maze software. A potential caveat is that sequential behavioral tests modifies performance (i.e., any differences observed in novel object recognition are related to LPS-driven performance deficits over 3 days of testing). We have attempted to minimize such an effect by staggering the tests from least to most complex or stressful (i.e., spontaneous alternation then novel object recognition with a 24 hr gap in-between) to minimize multitesting effects.

Spontaneous Alternation (Y-maze)

Mice were placed in the entry arm of a Y-maze apparatus ($38.5 \times 8 \times 13$ cm, spaced 120° apart) and allowed to explore freely for 10 min. The sequence of arm entries was recorded and spontaneous alternation calculated: number of alternations (three successive entries that include one instance in each arm) divided by the total possible alternations (number of arms entered minus 2) multiplied by 100.

Novel Object Recognition

Briefly, mice were habituated in a white testing arena ($33 \times 25 \times 12.5$ cm) for 10 min, allowed to rest in their home cage for 50 min, and then returned to the same testing arena for 10 min. After 24 hr, mice were placed

in the same testing arena with two identical objects for 10 min. After being returned to their home cage for 50 min, they were placed back into the testing arena containing a familiar and novel object for 10 min. The discrimination index (DI) was calculated as: $DI = \frac{(T_N - T_F)}{(T_N + T_F)}$, where T_N is the time spent exploring the novel object and T_F is the time spent exploring the familiar object.

Tissue Harvest

Twenty-four hours after the final injection of LPS, EFAD mice were injected i.p. with 200 μ l of 2% sodium fluorescein (NaFl, see below for quantification) in sterile ddH₂O and anesthetized 30 min later with ketamine (100 mg/kg) and xylazine (10 mg/kg). Following anesthetization, blood was drawn from the right ventricle of the heart using a heparin-coated needle and centrifuged at $1,500 \times g$ for 15 min at 4°C to collect the plasma. The plasma was analyzed immediately for NaFl extravasation or snap frozen in liquid nitrogen and stored at -80°C .

Mice were then transcardially perfused with PBS containing protease inhibitors (Millipore, Darmstadt, Germany) at a rate of 4 ml/min for 5 min. Dissected left hemi-brains were frozen in Optimal Cutting Temperature (OCT) and stored at -80°C until immunohistochemical (IHC) analysis. Right hemi-brains were further dissected into the cortex, hippocampus, and cerebellum, weighed,

homogenized in PBS, and processed immediately for NaFl extravasation. A fraction of each PBS brain region homogenate was reserved for biochemical analysis.

NaFl Extravasation Analysis

PBS homogenates were resuspended in equal volumes of 60% trichloroacetic acid, vortexed, and centrifuged at $18,000 \times g$ for 10 min at 4°C . The supernatant was collected and fluorescence was read using a SpectraMax i3x microplate reader (Molecular Devices). Cleared volume of NaFl that passed from the plasma into the brain was calculated as follows:

$$\text{Cleared Volume} = \frac{\frac{\text{Brain Fluorescence (AU)}}{\text{Plasma Fluorescence (AU}/\mu\text{l})}}{\text{Brain Weight (mg)}}$$

Biochemical Analysis

Reserved aliquots of PBS extracts from homogenized brain tissue (see NaFl analysis protocol) were further processed using a modified version of the three-step extraction protocol described in Youmans et al. (2012a) in order to separate soluble, detergent-soluble, and extracellular proteins. This protocol was developed to assess soluble $\text{A}\beta$ levels (considered particularly AD-relevant) and to fully extract total $\text{A}\beta$ (which is primarily driven by formic acid levels). In addition, the collection of a detergent soluble fraction enables subsequent analysis of neuronal proteins by Western blot analysis. Briefly, the PBS extracts were centrifuged ($100,000 \times g$ for 1 hr at 4°C), and the PBS-soluble supernatant was collected, snap frozen in liquid nitrogen, and stored at -80°C until use. The pellet was washed in Tris-buffered saline (TBS) and resuspended in TBS with 1% Triton X-100 (TBS-X), incubated at 4°C for 30 min with gentle rotation, and centrifuged ($100,000 \times g$ for 1 hr at 4°C). The TBS-X-soluble fraction was collected and frozen as described for the PBS extract. The remaining pellet was washed with TBS-X and resuspended in 70% formic acid (FA), incubated with gentle rotation at room temperature for 2 hr with occasional vortexing, and centrifuged ($100,000 \times g$ for 1 hr at 4°C). The FA-soluble supernatant was neutralized with 20 volumes of 1 M Tris base, aliquoted, and snap frozen in liquid nitrogen. Total protein in the PBS and TBS-X extracts was quantified using the PierceTM BCA Protein Assay Kit (Thermo Fisher). The ready-to-use Bradford reagent (Bio-Rad) was used to quantify total protein in the neutralized FA extract.

Western Blotting

Samples were loaded onto gels to allow comparison of LPS-treated groups against their appropriate PBS vehicle

controls (e.g., E4FAD + LPS vs. E4FAD + PBS) with an $n \geq 6$ of each group per gel. All samples were normalized to actin. Given the larger volume of cortical samples, we were able to run all of the PBS-treated vehicle controls together on four separate gels ($n = 6$ per group), in order to compare protein levels as a ratio of the E3FAD– PBS group. The limited volume of the hippocampal samples prevented us from running samples on the multiple gels required to plot the data as a ratio of the E3FAD– PBS group, as was conducted for cortex samples (i.e., there were only sufficient sample volumes to run a gel comparing PBS- to LPS-treated mice within a genotype, e.g., E4FAD– mice, but not to run separate gel(s) with all the PBS samples across genotypes, i.e., comparing samples from E3FAD–, E3FAD+, E4FAD–, E4FAD+ mice). TBS-X fractions from the three-step extraction were analyzed for neuronal proteins and actin by western blot as described previously (Thomas et al., 2016). Briefly, protein ($15 \mu\text{g}$ for cortex, $10 \mu\text{g}$ for hippocampus) was separated on 4% to 12% Bis-Tris gels (Invitrogen), transferred onto low-fluorescence PVDF, blocked with 5% milk in 0.1% Tween-20 in TBS (TBS-T), and probed with primary antibody in 5% bovine serum albumin (BSA): overnight at 4°C for postsynaptic density-95 (PSD-95, 1:1000, Cell Signaling) and synaptophysin (1:1000, Cell Signaling); 1 hr at room temperature for actin (1:20000, Cell Signaling). After washing (3×5 min, TBS-T), membranes were incubated for 1 hr in the appropriate secondary antibody (Jackson ImmunoResearch). Proteins were imaged and quantified using the Odyssey[®] Fc Imaging System and normalized to actin. Actin-normalized LPS-treated groups are expressed as either a ratio of the E3FAD– PBS-treated group (cortex) or as a ratio of their own PBS-treated vehicle controls (hippocampus).

Enzyme-Linked Immunosorbent Assay

ApoE and $\text{A}\beta_{42}$ were measured by enzyme-linked immunosorbent assay (ELISA) in the PBS, TBS-X, and FA extracts. The apoE ELISA was performed as described in Tai et al. (2014) using anti-apoE (1:2000, Millipore) and biotinylated anti-apoE (1:5000, Meridian) for capture and detection antibodies, respectively. $\text{A}\beta_{42}$ was measured by a commercially available ELISA kit following the manufacturer instructions (Life Technologies).

Fluorescent IHC

Laminin and $\text{A}\beta$ IHC analysis was conducted as previously described in Thomas et al. (2016). Succinctly, sagittal sections were taken beginning at the stereotaxic coordinate of ML 3.72 mm through 0 mm in order to encompass the cortex and the entire hippocampal formation. Nine nonadjacent, $12 \mu\text{m}$ frozen sections ($192 \mu\text{m}$ apart) per animal were fixed with 10% neutral buffered

formalin (Sigma). Incubation in FA is a frequently utilized method for antigen retrieval of A β and, therefore, was performed here (Kitamoto et al., 1987; Cummings et al., 2002; Christensen et al., 2009; Youmans et al., 2012a; Youmans et al., 2012b; Thomas et al., 2016). Following antigen retrieval (52.8% FA, 8 min, room temperature), sections were permeabilized with 0.25% Triton X-100 in TBS (dilution media), blocked in 5% BSA in dilution media, and incubated in primary antibody overnight at 4°C in a humidified chamber. Anti-A β (MOAB-2, mouse IgG_{2b}, 1:250, Biosensis) and anti-laminin (rabbit, 1:200, Abcam) primary antibodies were diluted in 2% BSA and 0.1% Triton X-100 in TBS. Next, sections were washed 3 \times 5 min in dilution media and incubated in the appropriate Alexa fluorophore-conjugated secondary antibodies (1:200, AlexaFluor 350 anti-mouse IgG_{2b}, AlexaFluor 750 anti-rabbit, Invitrogen) in 2% BSA and 0.1% Triton X-100 in TBS, followed by 3 \times 5 min washes in dilution media, and 1 \times 5 min in TBS. Mosaic¹ and single images were obtained at 20 \times magnification on a Zeiss Axio Imager M1 under identical exposure settings and equally thresholded on ImageJ software (NIH, ImageJ). Laminin and A β levels were quantified in the full cortex, deep layer cortex, and subiculum using the “Analyze Particles” feature. Brain regions of interest were standardized with reference to the Allen Mouse Brain Atlas. Specifically (see Supplementary Figure 1(a)), the cortex included all six layers of the isocortex, whereas the deep layer cortex included only layers 2/3 through 6a of the isocortex. The subiculum was traced for each section excluding other regions of the retrohippocampal region (i.e., the entorhinal area, the parasubiculum, the postsubiculum, and the presubiculum).

Cerebral amyloid angiopathy (CAA)-like deposition was quantified as described in (Tai et al., 2017). Briefly, mosaic images contained for A β (MOAB-2) and laminin were captured using identical settings at 20 \times magnification as described for vessel coverage. Converted images were thresholded equally and quantified using the “Colocalization Threshold” feature in NIH ImageJ software.

Tissue sections for confocal microscopy and 3D vessel reconstruction were sectioned as described earlier. Tissue was probed with anti-A β (MOAB-2, mouse IgG_{2b}, 1:250, Biosensis) and anti-laminin (rabbit, 1:200, Abcam) or anti-CD31 (rat, 1:10, BD Bioscience) followed by the appropriate secondary (1:200, AlexaFluor 350 anti-mouse IgG_{2b}, AlexaFluor 555 anti-rabbit, AlexaFluor 594 anti-rat, Invitrogen). Representative Z-stack images of cortical vessels with overlapping fluorescence for A β and laminin or CD31 were taken at 63 \times magnification on a Zeiss LSM 710 Confocal Microscope. Imaris 7.7.2 software was used to produce 3D vessel reconstructions and visualize CAA in the cortical cerebrovasculature.

Multiplex Analysis of Peripheral Cytokines

Plasma cytokine levels were measured using a Bio-Plex ProTM Mouse Cytokine 23-plex Assay (Bio-Rad) according to the manufacturer protocol. For quantification, standard curves were generated using standards for each cytokine (included in the kit) and analyzed using a five-parameter logistic equation. Sample concentrations were calculated based on parameters obtained using the standard curve. Hierarchical cluster analysis was performed using Cluster 3.0 (de Hoon et al., 2004) and visualized using Java Treeview (Saldanha, 2004) software.

Statistical Analysis

Sample sizes were as follows: E3FAD–PBS ($n=9$), E3FAD–LPS ($n=7$), E3FAD+PBS ($n=7$), E3FAD+LPS ($n=7$), E4FAD–PBS ($n=10$), E4FAD–LPS ($n=11$), E4FAD+PBS ($n=9$), and E4FAD+LPS ($n=12$). All samples were utilized for analysis unless stated in the results. For IHC analysis $n=6$ for all groups.

A mixed model was used to analyze changes in body-weight over time and between treatments. The random intercepts and slopes model included linear time, treatment, and their interaction as fixed effects. Overall effects were analyzed by inverse-variance-weighted three-way analysis of variance (ANOVA), testing initially for mean differences using the omnibus F test with a saturated model. Post hoc mean comparisons driven by visual inspection of the results were conducted using the appropriate orthogonal contrasts with Bonferroni’s correction. Three-way ANOVA and post hoc analysis were carried out with R version 3.3.0 (R Core Team, 2014). Weighted two-way ANOVA with Bonferroni’s correction and Student’s t -test analyses were conducted using GraphPad Prism Version 6. All data are represented as the mean \pm standard error (SEM).

Results

Systemic LPS Administration Induces Cognitive Dysfunction in E4FAD+ Mice

The overarching goal of this study was to determine the interactive effects of chronic repeated peripheral inflammation, *APOE*, and A β on cerebrovascular and AD-like pathology *in vivo*. Wild-type mice were excluded from this study as mouse apoE is structurally distinct from each of the human apoE isoforms. Human apoE isoforms differ by a single amino acid change at residues 112 and 158 (apoE3^{Cys,Arg}, apoE4^{Arg,Arg}), whereas mouse apoE is expressed as a single isoform and differs from all human apoE isoforms by approximately one third of its nearly 300 amino acids (Tai et al., 2017). The structural differences result in unique functional effects of mouse

apoE compared to the human apoE isoforms. Therefore, mouse models were developed to enable a comparison of human *APOE3* to human *APOE4* and to mimic more closely *APOE4*-induced AD risk in humans. To incorporate *APOE* and A β , EFAD mice were employed, which express human *APOE3* (E3FAD mice) or *APOE4* (E4FAD mice) and overproduce A β 42 via the 5xFAD mutations (Youmans et al., 2012a). Male EFAD carrier [5xFAD^{+/-}/*APOE*^{+/+} (EFAD+)] and noncarrier [5xFAD^{-/-}/*APOE*^{+/+} (EFAD-)] mice expressing *APOE3* or *APOE4* were utilized in order to dissect the effects of peripheral inflammation in the presence and absence of high levels of human A β . For peripheral inflammation, EFAD mice were treated with LPS, a bacterial endotoxin, and toll-like receptor 4 agonist commonly utilized to induce an inflammatory response. We selected a low dose (0.5mg/kg i.p.) reported to be the threshold of physiological changes (Vaure and Liu, 2014) and only treated mice once a week to achieve a repeated low-level peripheral inflammatory response. Thus, male EFAD+ and EFAD- mice were treated from 4 to 6 months of age (Figure 1(a), LPS, 0.5mg/kg/wk i.p.) to start at an age of initial A β deposition and prior to cognitive deficits (Youmans et al., 2012a; Thomas et al., 2016).

There were no changes in bodyweight after LPS treatment regardless of *APOE* genotype (Figure 1(b), $F(1, 67) = 1.97$, $p > .05$). Further, we monitored EFAD+ and EFAD- mice continually over the treatment course and there were no overt signs of toxicity, i.e., death rates (none), fur loss, or wounds. Therefore, no characteristics of sickness behavior were observed, which are frequently associated with higher LPS doses and indicates acute, rather than chronic low-level inflammation.

Initially, the effect of LPS on cognition was assessed. As described in the “Materials and Methods” section, statistical analysis was conducted using a three-way ANOVA F test, to determine whether there were significant differences between any groups. Subsequent post hoc analysis was based on hypotheses derived from the scientific interpretation of the graphs, which for behavior and PSD-95 (see below) was focused on comparisons for LPS- and PBS-treated mice within each group. A similar approach was conducted for all three-way ANOVA comparisons throughout the study. LPS treatment had no effect on spatial memory as assessed by spontaneous alternation (Figure 2(a), $p > .05$). However, the novel object recognition test illuminated dysfunction in recognition memory in LPS-treated E4FAD+ mice compared to PBS-treated E4FAD+ mice (Figure 2(b), $F(7, 64) = 4.7$, $*p < .05$, followed by Bonferroni post hoc analysis comparing PBS- with LPS-treated mice within each group). Furthermore, no other groups demonstrated a deficit in recognition memory when challenged with LPS- compared to their own PBS-treated vehicle control.

Thus, repeated peripheral LPS challenge resulted in a substantial cognitive deficit in E4FAD+ mice.

Next, levels of PSD-95 were assessed by western blot analysis. The extraction procedure utilized in this study resulted in higher cortical volumes for western blot analysis. Thus, as described in the “Materials and Methods” section, we were able to plot expression levels (normalized to actin) as a ratio of the PBS-treated E3FAD- group. There were higher levels of PSD-95 in the cortex of LPS- compared to PBS-treated E3FAD+ (Figure 2(c), $F(7, 62) = 7.6$, $*p < .05$, followed by Bonferroni post hoc analysis comparing PBS- with LPS-treated mice within each group). These data indicate an adaptive, potentially protective response. Consistent with the behavioral deficits, there was a nonsignificant trend in which, compared to PBS, LPS treatment resulted in lower levels of the postsynaptic protein PSD-95 in the cortex of E4FAD+ mice (Figure 2(c); $p = .088$). Due to volume restrictions in the hippocampal samples, we could only compare the LPS- and PBS-treated groups (Student’s t -test). LPS treatment resulted in lower PSD-95 levels only in E4FAD+ mice, with ~25% lower levels compared to PBS-treated E4FAD+ mice. There were no significant differences in the levels of the presynaptic protein synaptophysin for any of the groups (data not shown). Collectively, these data support that LPS treatment from 4 to 6 months of age induces cognitive deficits and lowers PSD-95 levels in E4FAD+ mice.

Higher Cerebrovascular Leakiness and Lower Vessel Coverage in LPS-Challenged E4FAD+ Mice

To determine the roles of peripheral inflammation and *APOE* in cerebrovascular integrity, we first measured NaFl levels in the brain following i.p. injection (Figure 3). Cortical NaFl levels were significantly higher in LPS-treated, compared to PBS-treated, E4FAD+ mice (Figure 3(a); $F(7, 55) = 4.2$, $*p < .05$ followed by Bonferroni post hoc analysis comparing PBS- with LPS-treated mice within each group; insufficient plasma volumes due to imperfect blood draws resulted in the prioritization of samples for later multiplex analysis and exclusion from NaFl analysis: E3FAD- PBS ($n = 6$), E3FAD- LPS ($n = 6$), E3FAD+ PBS ($n = 7$), E3FAD+ LPS ($n = 6$), E4FAD- PBS ($n = 10$), E4FAD- LPS ($n = 7$), E4FAD+ PBS ($n = 9$), and E4FAD+ LPS ($n = 12$)). Indeed, cortical NaFl levels were ~300% higher in E4FAD+ mice treated with LPS. There were no other differences when comparing PBS- to LPS-treated mice within any other group. In the hippocampus, LPS treatment did not significantly increase NaFl levels compared to the PBS-treated mice in any group (Figure 3(b); $p = .07$). Lack of an effect for LPS in E4FAD+ mice in the hippocampus may be related to the lower signal-to-noise ratio of the hippocampus.

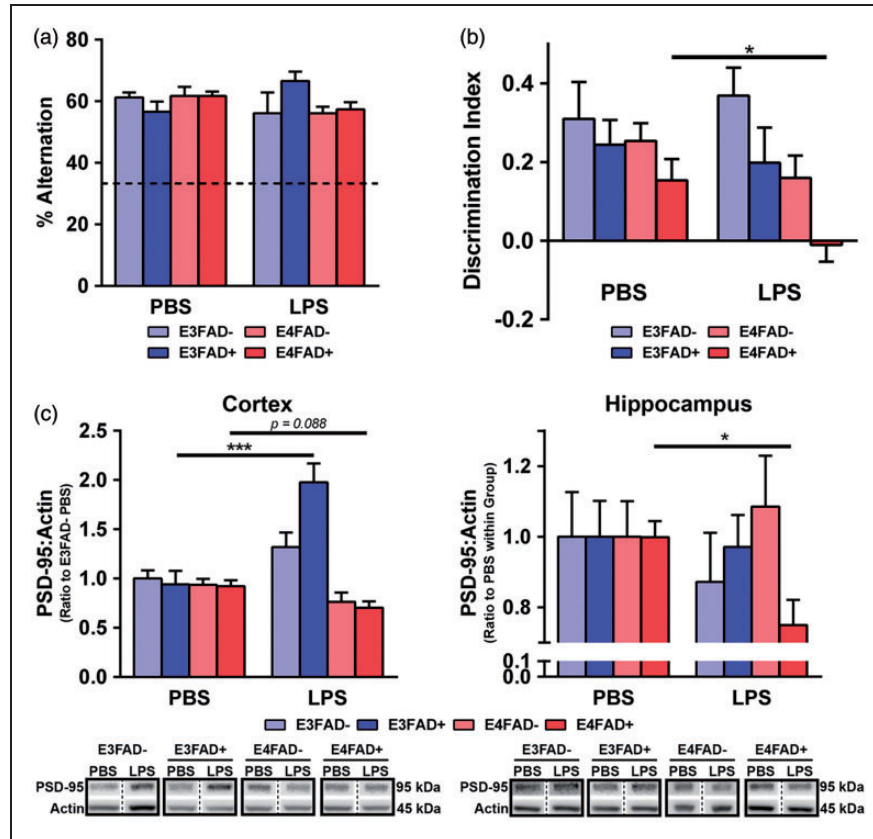


Figure 2. Cognitive dysfunction in LPS-treated E4FAD⁺ mice. (a) Spatial memory was unaffected by LPS treatment when assessed by spontaneous alternation (Y-maze). (b) LPS-induced recognition memory deficits in LPS-treated E4FAD⁺ mice compared to PBS-treated E4FAD⁺ mice. (c) In the cortex, post-synaptic density-95 (PSD-95) protein levels (normalized to actin) were higher in E3FAD⁺ mice treated with LPS compared to PBS, indicating a potential adaptive response. In the cortex, there was a nonsignificant trend where, compared to PBS, LPS treatment resulted in lower levels of PSD-95 of E4FAD⁺ mice. In the hippocampus, E4FAD⁺ mice treated with LPS had lower PSD-95 levels compared to PBS-treated mice. Solid black boxes indicate samples were run on the same gel; bands on the same gel in nonadjacent positions are separated by a dashed line. Data are expressed as the mean \pm SEM. * $p < .05$ by three-way ANOVA followed by Bonferroni post hoc analysis comparing PBS- with LPS-treated mice within each group. The exception is for PSD-95 levels in the hippocampus for (c) where * $p < .05$ by *t*-test.

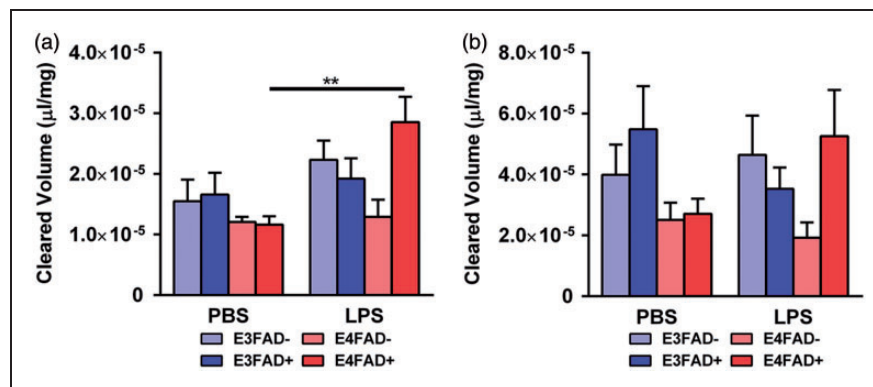


Figure 3. Higher cerebrovascular leakiness in LPS-treated E4FAD⁺ mice. (a) When assessed by sodium fluorescein (NaFl) extravasation, peripheral administration of LPS resulted in 300% higher cortical NaFl levels in E4FAD⁺ mice compared to PBS. (b) In the hippocampus, no differences were observed between LPS and PBS groups. Data are expressed as the mean \pm SEM. * $p < .05$ by three-way ANOVA followed by Bonferroni post hoc analysis comparing PBS- with LPS-treated mice within each group.

Total vessel coverage is an indication of a disrupted cerebrovasculature, and at 8 months of age, we have observed lower vessel coverage in the subiculum and deep layer cortex of female E4FAD+ mice compared to age-matched males (Thomas et al., 2016). The region-specific lowering of vessel coverage is likely driven by the accumulation of A β in those regions of EFAD+ mice and increased susceptibility of vessels to damage (see “Discussion” section). Therefore, the effects of LPS on cerebrovascular coverage were assessed using a staining for laminin, a basement membrane protein, in the full cortex, deep layer cortex, and subiculum (see Supplementary Figure 1(a) for a representative image of brain regions used for quantification), to match our previous study in female EFAD mice. Laminin coverage in the deep layer cortex and subiculum qualitatively appeared lower in E4FAD+ mice that had been treated with LPS compared to PBS (Figure 4(a, b)). Quantification revealed that, in E4FAD+ mice treated with LPS compared to PBS, vessel coverage was 25% lower in full and deep layer cortex and ~35% lower in the subiculum ($F(7, 40) = 3.30, 9.78, 13.35$ for each brain region, respectively, $*p < .05$, followed by Bonferroni post hoc analysis comparing PBS- with LPS-treated mice within each group). The only other group that exhibited significantly lower vessel coverage in the subiculum with LPS versus PBS treatment was E4FAD– mice. These data indicate subtle cerebrovascular deficits in E4FAD– mice after repeated peripheral inflammation that may manifest as cognitive decline with longer treatment. Thus, LPS induces cerebrovascular deficits, including lower cerebrovascular coverage, in male E4FAD+ mice.

Higher Extracellular A β in the Cortex of LPS-Treated E4FAD+ Mice

EFAD+ mice serve as a model of *APOE*-modulated A β levels and induced dysfunction, with A β pathology primarily in the subiculum of the hippocampal formation and in the deep layers of the frontal cortex. Therefore, we assessed whether repeated peripheral challenge with LPS had an effect on brain A β 42 levels biochemically and by IHC (Figure 5(a) to (c)). As EFAD– mice were not assessed for A β , statistical analysis was conducted by two-way ANOVA followed by Bonferroni post hoc analysis. In the cortex, there were no changes in soluble or total A β 42 levels when assessed biochemically (Figure 5(a), $F(1, 33), p > .05$, see Supplementary Figure 1(b) for full extraction profile). Since total A β consists primarily of extracellular A β , quantitative IHC analysis was conducted. There was a genotype effect ($F(1, 20) = 21.2, *p < .05$), and post hoc analysis revealed higher levels of A β in the cortex of LPS-treated E4FAD+ mice compared to LPS- and PBS-treated E3FAD+ (Figure 5(c), Bonferroni post hoc comparisons comparing

all groups). We are careful not to over interpret, due to the difficulty in distinguishing plaque size and number, but the higher percentage area covered by extracellular A β in the cortex of LPS-treated E4FAD+ mice was primarily driven by large size (Supplementary Figure 1(d), ($F(1, 20) = 17.8$ for genotype and treatment interaction, $*p < .05$, Bonferroni post hoc comparisons comparing all groups). As there were no differences by *APOE* genotype in the PBS group by IHC, these data indicate that LPS increased insoluble A β levels in the cortex of E4FAD+ mice. The partial differences between the IHC and biochemical data may be related to the relatively high variation of A β levels in the E4FAD+ PBS group; however, visually, the graphs followed the same trend. In the hippocampus, there was both a genotype ($F(1, 33) = 16.64, *p < .05$) and a treatment interaction ($F(1, 33) = 8.190, *p < .05$), with higher levels of soluble A β (PBS extraction) in the hippocampus of LPS-treated E4FAD+ mice compared to all other groups (Figure 5(b), Bonferroni post hoc comparisons comparing all groups, see Supplementary Figure 1(c) for full extraction profile). Although no differences were observed for total A β 42, extracellular A β primarily deposits in the subiculum of EFAD+ mice, which may have partially confounded biochemical analysis of the entire hippocampus. We therefore quantified extracellular A β in the subiculum by IHC. Similar to the cortex, there was a genotype effect in the subiculum ($F(1, 20) = 13.06, *p < .05$) with higher levels of A β for LPS-treated E4FAD+ mice compared to E3FAD+ mice treated with LPS (Figure 5(c), Bonferroni post hoc comparisons comparing all groups). However, there were no differences for any treatments or genotypes in extracellular A β deposit size or count (Supplementary Figure 1(e)).

ApoE was also measured by ELISA in both the cortex and the hippocampus to determine if LPS modulated apoE levels.² When each fraction was assessed separately, significance in the *F* test was only reached for the soluble (PBS) fraction in the cortex ($F(7, 58) = 5.0, *p < .05$) and the hippocampus ($F(7, 54) = 5.5, *p < .05$). To dissect the changes, we conducted post hoc analysis comparing the different genotypes within the PBS or LPS treatments and PBS versus LPS treatments within groups (with simultaneous analysis using Bonferroni correction). Post hoc analysis demonstrated that there are lower apoE levels in E4FAD– mice treated with PBS compared to E3FAD– mice treated with PBS. However, there were no effects of LPS treatment on apoE levels compared to PBS controls for any of the groups.

Therefore, LPS induced mixed effects on A β levels for E4FAD+ mice: higher soluble A β levels in the hippocampus biochemically, and, by IHC, higher extracellular A β in the cortex and subiculum.

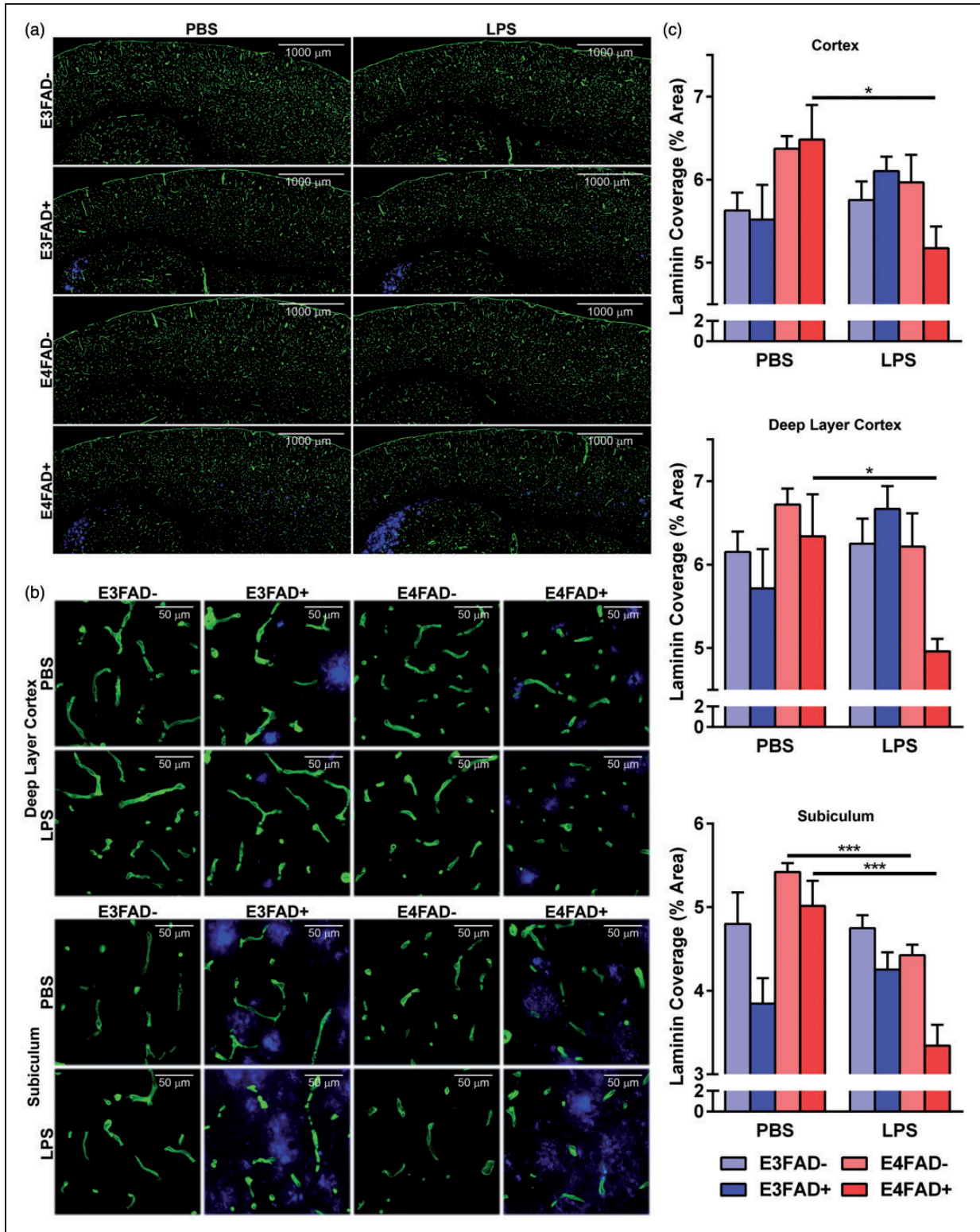


Figure 4. Lower vessel coverage in LPS-treated E4FAD+ mice. (a) Composite mosaic images stitched together from images taken at 20× magnification. (b) 20× representative images of 12 μm brain sections costained for laminin (green, a basement membrane protein) and extracellular Aβ (blue, IHC using antibody MOAB2). Vessel coverage is visually lower in LPS-challenged E4FAD+ mice. (c) When quantified laminin coverage was significantly lower in E4FAD+ mice treated with LPS in both the deep layer of the cortex and the subiculum compared to PBS treatment. In addition, in the subiculum of E4FAD- mice, there is lower vessel coverage in LPS- compared to PBS-treated mice. Data are expressed as the mean ± SEM. **p* < .05 by three-way ANOVA followed by Bonferroni post hoc analysis comparing PBS- with LPS-treated mice within each group.

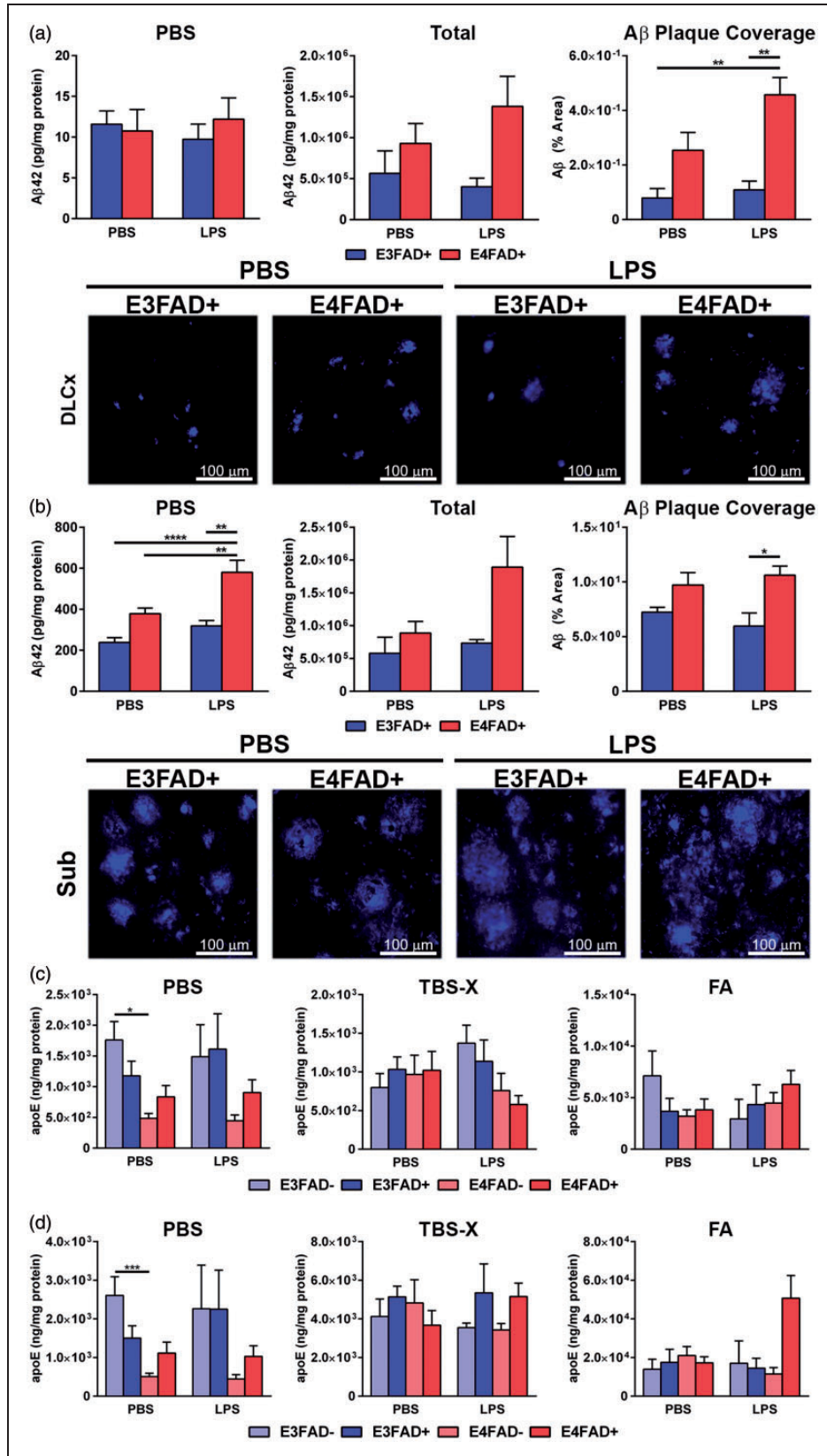


Figure 5. LPS increases Aβ42 levels in E4FAD+ mice. (a) In the cortex, there were no changes in soluble (left panel) or total Aβ42 levels (center panel) when assessed biochemically. Total Aβ is the sum of the amount of Aβ in every fraction divided by the protein content in

Higher CAA-Like A β Deposition in E4FAD+ Mice

Given that extracellular A β 42 levels appeared higher in LPS-challenged E4FAD+ mice and the fact that A β can deposit in the vasculature, CAA-like deposition was assessed (laminin-A β costain). Despite the abundance of A β plaques in the subiculum, CAA-like deposition was only evident in the cortex (Figure 6(a)). CAA was higher in LPS-treated E4FAD+ mice compared to PBS- and LPS-treated E3FAD+ mice (Figure 6(b), two-way ANOVA, $F(1, 20)=23.91$, $*p < .05$, followed by Bonferroni post hoc comparisons comparing all groups). These data support that CAA is highest in LPS-treated E4FAD+ mice. Next, we assessed the localization of deposited A β using confocal microscopy followed by 3D reconstruction of the basement membrane (laminin), vessels (CD31), and A β (Figure 6(c) to (e)). In E4FAD+ LPS-treated mice, A β was localized within the laminin basement membrane in both larger vessels (Figure 6(c)) and capillary-like vessels (Figure 6(d)). Costaining of CD31-labeled vessels and A β confirmed that the amyloid deposition was not within the endothelial cells (Figure 6(e)). We therefore determined that CAA-like deposition of A β was outside of the brain endothelial cells within the basement membranes surrounding vessels of various diameters and is potentially higher in LPS-treated E4FAD+ mice.

Plasma Cytokine Levels Are Modulated by APOE Genotype and LPS Treatment

To dissect whether LPS induced a differential response in peripheral inflammation for the different groups, plasma levels of 23 cytokines/chemokines were assessed by multiplex analysis. Our focus was on cytokines/chemokines whose levels remained changed over a longer time period after each LPS treatment, rather than acute differences. Therefore, we waited 24 hr after the last LPS injection to assess cytokine/chemokine levels. In general, cytokine levels were varied within each group, likely due to the time point selected for analysis, as typically cytokines are assessed within an hour of LPS injection (i.e., high levels). However, hierarchical cluster analysis

of the complete data set (i.e., significant and nonsignificant differences) revealed that LPS induced a number of potentially interesting changes (Figure 7(a)). Overall, there was a cluster (C1) of chemokines (macrophage inflammatory protein [MIP]-1) and pro-inflammatory cytokines (interleukin [IL]-6, IL-5, and tumor necrosis factor [TNF]- α) whose levels were similar for all PBS-treated groups, but were increased by LPS. A second cluster (C2) increased in levels with LPS in E4FAD+ and E4FAD- mice and included chemokines (regulator on activation, normal T cell expressed and secreted (RANTES), granulocyte-colony stimulating factor (G-CSF)) and cytokines whose function can be pro- or anti-inflammatory depending on context (IL-1 α , IL-10). In addition, cytokines/chemokines in a third larger cluster (C3) were higher in E3FAD+ or E3FAD- compared to E4FAD+ or E4FAD- in the PBS group and remained high, or were lower in the LPS-treated mice. C3 included both pro- and anti-inflammatory cytokines.

We further dissected the data based on significantly different changes, which reduced the overall number of cytokines. Although there were changes in some cytokines/chemokines regardless of APOE or FAD status (e.g., IL-6, MIP-1 α in C1), we have focused on differences between APOE3 and APOE4, due to the cognitive and cerebrovascular dysfunction in E4FAD+ mice treated with LPS. In C2, there was significance by F test for IL-10 ($F(7, 59)=2.5$, $*p < .05$) and RANTES ($F(7, 64)=6.8$, $p < .05$). Visually, the differences appeared driven by increased plasma levels of IL-10 and RANTES in mice that express APOE4 (i.e., E4FAD+ and E4FAD-) treated with LPS compared to PBS (Figure 7(b)). These changes were significant using Bonferroni post hoc analysis that compared PBS to LPS treatments for the grouped averages of APOE4 (i.e., E4FAD+ and E4FAD-) or APOE3 (i.e., E3FAD- and E3FAD+). In addition, although not significant by F test, a post hoc analysis revealed the same effect for G-CSF (i.e., LPS increased plasma levels in mice that express APOE4 [E4FAD- and E4FAD+ averaged] but not APOE3). For cytokines in C3, there was also a genotype effect, but in the PBS groups.

Figure 5. Continued

every fraction. As total A β primarily consists of extracellular A β , quantitative IHC analysis was conducted (right panel and images). There were higher levels of A β in the cortex of LPS-treated E4FAD+ mice compared to LPS- and PBS-treated E3FAD+ mice. (b) In the hippocampus, there were higher levels of soluble A β (PBS extraction) in the hippocampus of LPS-treated E4FAD+ mice compared to all other groups. Although no differences were observed for total A β 42, when extracellular A β in the subiculum was quantified by IHC, there were higher levels in LPS-treated E4FAD+ mice compared to E3FAD+ mice treated with LPS. (c) For apoE, the only significant differences were in the soluble (PBS) extracts with lower apoE levels in E4FAD- mice treated with PBS compared to E3FAD- mice treated with PBS. However, there were no effects of LPS treatment on apoE levels compared to PBS controls for any groups. Data are expressed as the mean \pm SEM. (a, b) $*p < .05$ by two-way ANOVA followed by Bonferroni post hoc analysis (c, d) $*p < .05$ by three-way ANOVA followed by Bonferroni post hoc analysis comparing all groups.

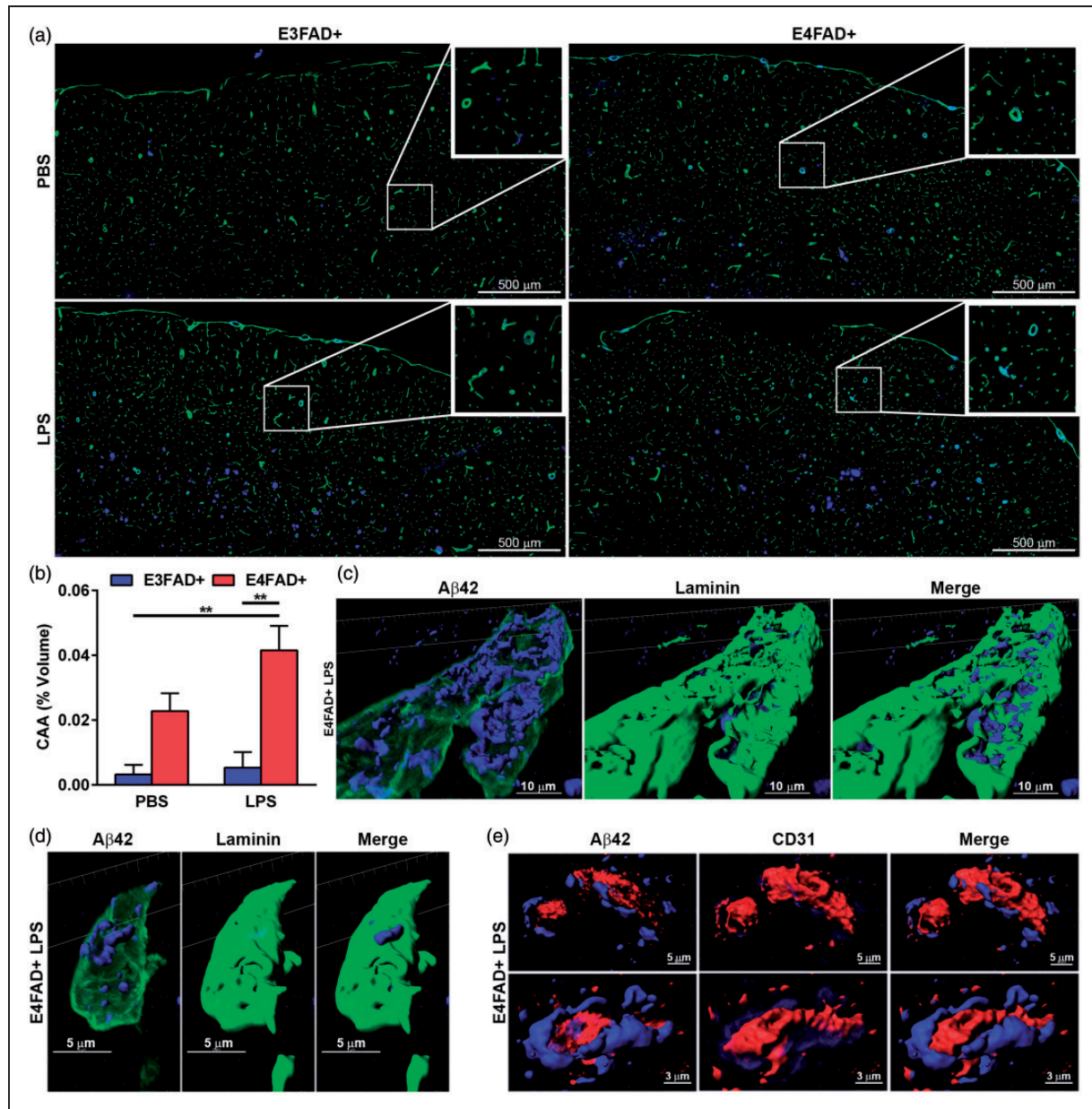


Figure 6. CAA-like deposition is higher in E4FAD+ mice. (a) Mosaic images of 12 μm sections costained for laminin (green) and A β (blue) stitched together from individual 20 \times images. (b) Quantification of A β -laminin costaining. (c to e) 3D reconstruction from 63 \times confocal image of a cortical (c) larger vessels or (d, e) capillary stained for A β (blue) and (c, d) laminin (green) or (e) CD31 (red) indicating that CAA-like deposition is outside of the blood vessel within the basement membrane. (b) * $p < .05$ by two-Way ANOVA followed by Bonferroni post hoc comparisons comparing all groups.

Our analysis for the cytokines in C3 was based on the representation of the data that indicated a genotype effect in the PBS group (Figure 7(c)). In the PBS group, IL-17 and IL-12(p70) levels were higher when the average value for mice that express *APOE3* (E3FAD- and E3FAD+) was compared to the average of mice that express *APOE4* (E4FAD- and E4FAD+) (with Bonferroni correction). In the LPS group, there were no *APOE* genotype differences (for IL-17 or IL-12(p70)). For CXCL1 (KC), there

was a genotype effect in the LPS group but not in the PBS group using a similar comparison, which suggests higher KC levels with *APOE3*. Therefore, in general for group C3, the cytokine/chemokine levels are lower with *APOE4* in the PBS group. As there were no specific differences in E4FAD+ mice treated with LPS compared to E4FAD- mice, the observed cytokine changes may contribute to, but not drive, the cerebrovascular impairments observed in E4FAD+ mice treated with LPS.

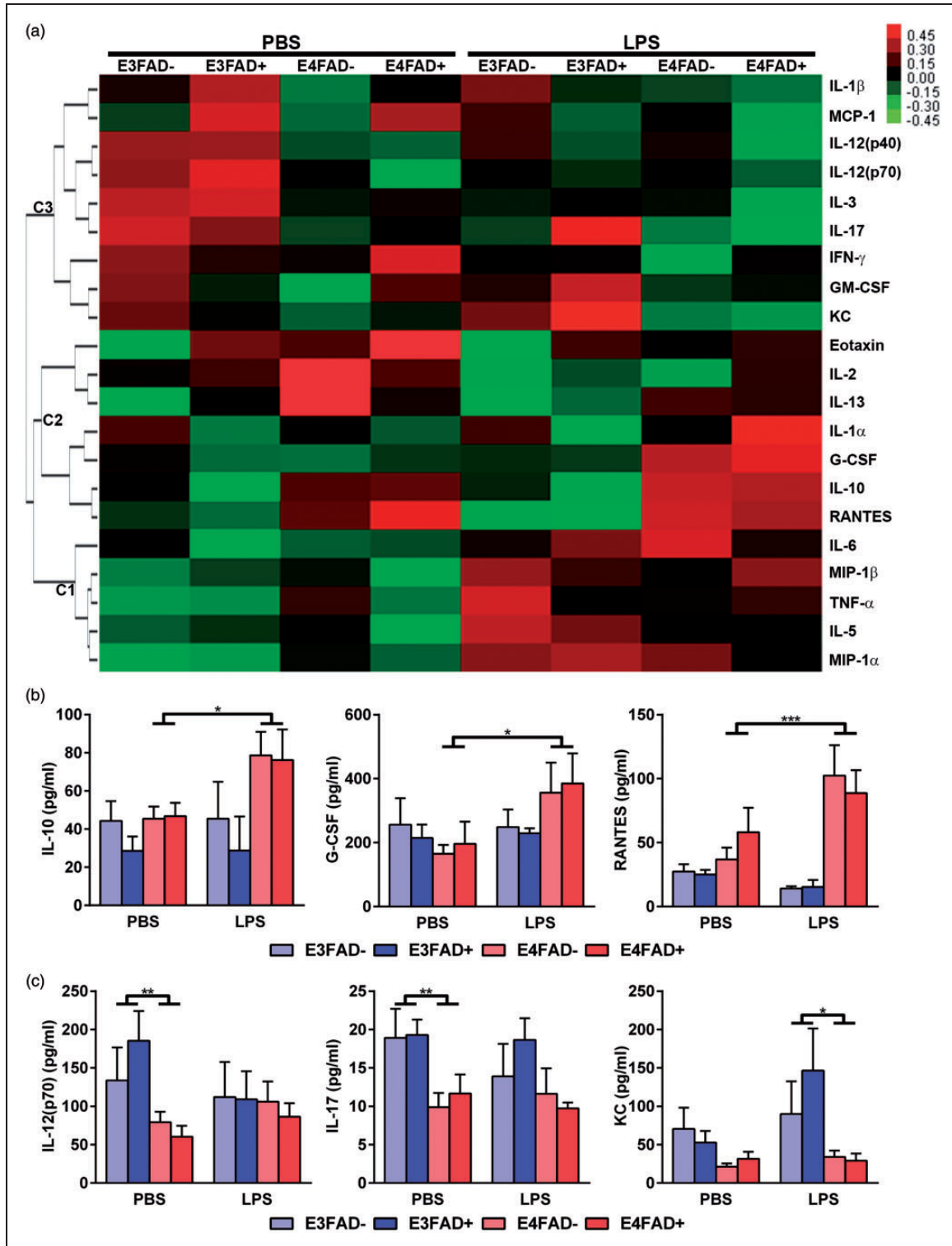


Figure 7. LPS induced various changes in peripheral cytokine levels. (a) Heatmap of peripheral cytokines indicating three hierarchical clusters. In C1, cytokine levels were generally increased by LPS. In C2, cytokine levels were generally lower following LPS treatment. C3 contained cytokines/chemokines that were higher in E3FAD+ or E3FAD- compared to E4FAD+ or E4FAD- in the PBS group and remained high, or were lower in the LPS-treated mice. (b) Cytokines that were similar in the VC group, but levels increased with *APOE4* following LPS treatment. (c) Cytokines whose levels were higher with *APOE3* compared to *APOE4* in PBS or LPS treatment groups. In (b), * $p < .05$ by three-way ANOVA followed by Bonferroni post hoc analysis comparing PBS to LPS treatments for the grouped averages of *APOE4* (i.e., E4FAD+ and E4FAD-) or *APOE3* (i.e., E3FAD- and E3FAD+). In (c), * $p < .05$ by three-way ANOVA followed by Bonferroni post hoc analysis comparing within PBS or LPS groups the values for mice that express *APOE3* (E3FAD- and E3FAD+) to mice that express *APOE4* (E4FAD- and E4FAD+).

Discussion

Increasing evidence supports that cerebrovascular dysfunction is a key component of AD; however, the role of known AD hits in cerebrovascular dysfunction is unclear. Here we demonstrate that peripheral inflammation, *APOE4*, and A β interact to induce cognitive and cerebrovascular dysfunction. Our ongoing studies are focused on validating and further dissecting the contrasts identified in this study.

The first important finding is that repeated peripheral challenge with LPS induces cognitive impairment in male E4FAD+ mice. Our data are partially consistent with previous studies where acute or extended, daily (3–7 days) LPS treatment induced cognitive deficits in mice and rats (Pugh et al., 1998; Shaw et al., 2001; Sparkman et al., 2005; Thomson and Sutherland, 2005) and exacerbated cognitive deficits in models of aging (Chen et al., 2008) and neurodegeneration (Cunningham et al., 2009; Joshi and Pratico, 2014). Further, human data suggest peripheral inflammation is linked to AD risk (Michaud et al., 2013) and cognitive function in aging (Marsland et al., 2015). However, our paradigm enabled us to delineate that repeated peripheral challenge with LPS, *APOE4*, and A β interact to induce cognitive deficits. For acute peripheral inflammation, there is evidence of worse functional (noncognitive) outcomes with *APOE4*. Acute LPS-induced hypothermia is greater with *APOE4* compared to *APOE3* in *APOE*-targeted replacement mice (that do not overproduce A β), and LPS-induced hyperthermia is greater with *APOE4* compared to *APOE3* in humans (Gale et al., 2014). Thus, there is a growing body of evidence supporting that *APOE4* and peripheral inflammation interact to induce detrimental functional responses. Future studies aimed at fully dissecting the temporal sequence of cognitive deficits in EFAD+ and EFAD– mice may reveal whether the peripheral inflammation-induced cognitive decline is specific for, or accelerated by, *APOE4* and A β .

As the interface between the blood and the brain, the cerebrovasculature is particularly susceptible to the detrimental effects of *APOE4*, A β , and peripheral inflammation. Thus, our second important finding is that peripheral inflammation induced cerebrovascular dysfunction in E4FAD+ mice. These data are consistent with *in vitro*, *in vivo*, and human data that peripheral inflammation (Candeias et al., 2012; Meredith et al., 2015), *APOE4*, and A β are individually associated with cerebrovascular dysfunction. Further, *APOE4* synergistically interacts with vascular (including cardiovascular) risk factors, which induce cerebrovascular dysfunction, to increase AD risk (reviewed in Tai et al., 2016). The specific changes with peripheral inflammation in E4FAD+ mice were higher cerebrovascular leakiness and lower vessel coverage. The lower vessel coverage in the subiculum and deep layer cortex of E4FAD+ mice treated with

LPS may be related to the accumulation of A β in those brain regions in EFAD+ mice. Indeed, the accumulation of A β in the deep layer cortex and subiculum of E4FAD+ mice likely induces a number of pathways (see below) that predispose the brain endothelial cells to damage in response to peripheral inflammation. Alternatively/in addition, the brain region-specific increased susceptibility of the cerebrovasculature to damage in E4FAD+ mice in response to LPS may be related to: (a) vessels in the deep layer cortex and subiculum being more sensitive to damage due to the greater distance from the larger blood vessels; (b) the nature of the vessels in those regions (e.g., capillary vessels may be in higher density in those brain regions); and (c) there is a differential gene expression profile in brain endothelial cells by brain region. Our ongoing studies are focused on developing the complex techniques required to assess this issue.

Although data from human patients support that *APOE4* and AD are associated with higher cerebrovascular permeability, data on vessel coverage are unclear. Lower vessel coverage/degenerated microvasculature is observed in AD patients (Bush et al., 1990; Hashimura et al., 1991; Bouras et al., 2006; Kitaguchi et al., 2007; Miyakawa, 2010) and in FAD-mice (Ujiiie et al., 2003; Meyer et al., 2008; Lee et al., 2012; Giannoni et al., 2016). Contrastingly, higher vessel coverage (potentially angiogenesis) is also observed by other studies in AD patients and *in vivo* (Boscolo et al., 2007; Biron et al., 2011; Cameron et al., 2012). Therefore, there is currently a debate on the significance of changes in cerebrovascular length in AD. One proposal is that AD pathways induce hypersprouting and tight junction disruption, which increase cerebrovascular permeability (Boscolo et al., 2007; Biron et al., 2011; Cameron et al., 2012). A counter argument is that lower cerebrovascular coverage contributes to AD progression by disrupting the complex transport and metabolic systems of the cerebrovasculature (Paris et al., 2004; Kitaguchi et al., 2007; Donnini et al., 2010; Jantaratnotai et al., 2011). Our data may be more consistent with pathological angiogenesis (Ambrose, 2016): AD hits disrupt brain endothelial cell signaling cascades that are considered angiogenic; however, rather than promoting angiogenesis, brain endothelial cells become disrupted resulting in vessel degeneration. The temporal sequence of this disruption leads to progressive brain endothelial cell degeneration and increased leakiness of the cerebrovasculature. Our ongoing studies are focused on defining the temporal sequence of brain endothelial cell dysfunction induced by AD hits.

A potential consequence of cerebrovascular damage is higher A β levels. Indeed, E4FAD+ mice appeared to have higher total levels of A β 42 when challenged repeatedly with systemic LPS. Higher permeability of the cerebrovasculature may lead to the extravasation of peripheral factors, including LPS, into the brain. LPS has

been demonstrated to alter amyloid precursor protein expression (Brugg et al., 1995; Hauss-Wegrzyniak et al., 1998), increase A β production (Lee et al., 2008; Kahn et al., 2012), and decrease A β clearance (Jaeger et al., 2009; Erickson et al., 2012). Higher A β levels may deposit in the vasculature as CAA. Indeed, LPS-treated E4FAD+ mice had higher A β accumulation in the basement membrane of both larger vessels and capillaries. In humans, CAA is observed in approximately 90% of AD brains (reviewed in Vinters, 1987) and is higher with *APOE4* (Shinohara et al., 2016), consistent with our *in vivo* findings. Here, our low sample number and volume did not permit assessments of amyloid precursor protein levels/processing or a detailed analysis of CAA localization. However, our ongoing studies are focused on the role of LPS in A β production, clearance, and CAA-like deposition.

An important question raised by this current study is what temporal changes in cytokines/chemokines were induced by repeated (weekly) low-dose LPS treatment? Potential outcomes include: (a) LPS induced weekly transient (likely over 24 hr) changes in plasma cytokines that were similar after every injection and were sufficient to induce cerebrovascular dysfunction; (b) Initial LPS treatments preconditioned the mice to a greater transient cytokine/chemokine response with subsequent injections; (c) There was a cumulative (i.e., chronic and sustained) detrimental cytokine/chemokine profile in the plasma during the course of the LPS treatment, in addition to acute transient changes; (d) A tolerance to LPS developed with multiple injections; (e) Cytokine/chemokine levels in the brain were altered which mirrored or were distinct from the plasma; and (f) *APOE* modulated one or all of the above responses. A limitation of this current study is that cytokine levels were not assessed at different time points in the plasma during treatment and, due to sample limitation, brain cytokine levels were not measured; both concerns are the focus of our ongoing studies. For example, for neuroinflammation, interesting questions include whether (a) direct or indirect (via cytokines/chemokines) LPS-induced activation of brain endothelial cells transmits cytokine into the brain (via transcytosis or cytokine production by brain endothelial cells); (b) cerebrovascular leakiness leads to LPS extravasation into the brain, glial activation and a modulated neuroinflammatory cytokine/chemokine profile that contributes to cognitive impairment; and (c.) the temporal relationship between neuroinflammation, cerebrovascular dysfunction, and cognitive impairment. Here, plasma cytokines/chemokines were measured 24 hr after the last injection. Twenty-four hours was selected as a time point to mimic slightly longer term cytokine/chemokine changes with LPS after repeated past stimulation intervals, rather than acute changes immediately after treatment. Our justification was that sustained cytokine changes may contribute to

cerebrovascular dysfunction over the 2-month period of LPS treatment. However, due to the time point selected, there was a mixed and varied response within groups.

We have focused the discussion on cytokines that significantly differed between *APOE3* and *APOE4* and therefore may contribute to the cerebrovascular deficits described earlier. We are careful not to over-interpret these results as immediate changes in cytokine levels may have eluded detection at 24 hr, and all the cytokines measured exert multiple cellular functional responses (e.g., T-cell response and macrophage activation). Two *APOE*-modulated cytokine clusters were identified. The first (C2; G-CSF, IL-10, and RANTES) included cytokines that were higher in LPS-treated mice that express *APOE4* (E4FAD+ and E4FAD- mice) compared to the PBS group. RANTES promotes angiogenesis (Wang et al., 2006; Matsuo et al., 2009; Suffee et al., 2012; Liu et al., 2015a), while G-CSF and IL-10 have been demonstrated to both protect/maintain and disrupt the vasculature (Kohno et al., 2003; Dace et al., 2008; Tura et al., 2010; Kawabe et al., 2011; Alexandrakis et al., 2015; Cates et al., 2015; Liu et al., 2015a, 2015b; Wei et al., 2017). Therefore, it is possible that the C2 cytokines initiated angiogenic signaling in E4FAD+ and E4FAD- mice, without maturing into stable vessels, or induced direct brain endothelial cell disruption in a chronic setting. In the second cluster (C3; IL-12(p70), IL-17, and KC), cytokine levels were higher with *APOE3* compared to *APOE4* in the PBS group, except for KC, which was higher in the *APOE3* LPS treatment groups. IL-17 and KC have both been reported to have pro-angiogenic effects (Pickens et al., 2010; Liu et al., 2011; Miyake et al., 2013; Wang et al., 2015). In contrast, IL-12 results in disruption of angiogenesis (Strasly et al., 2001; Zhou et al., 2016). Although we did not track peripheral cytokine differences longitudinally, it is possible that higher levels of IL-17 and KC in E3FAD+ and E3FAD- mice prior to an inflammatory insult confer a protective effect on the cerebrovasculature, which is absent in E4FAD+ and E4FAD- mice. It is important to note that no cytokine differences were observed between E4FAD+ and E4FAD- mice.

Mechanistically, *APOE4*, A β and peripheral inflammation modulate multiple processes that may interact to induce cognitive decline. The proximal mechanism(s) of how each AD hit individually impacts disease progression is complex. As an example, apoE4 may induce detrimental changes in apoE-containing lipoprotein structure, lipidation, stability, toxic apoE fragment production, apoE levels, apoE receptor recycling, and receptor activity in a number of cell types (reviewed in Tai et al., 2014). As a consequence of one or more of these proximal events, inter-linked processes in the periphery (cholesterol metabolism and inflammation) and brain (lipid homeostasis, neuronal function, glucose metabolism, neurogenesis, tau phosphorylation, neuroinflammation, A β levels) are modified.

Thus, apoE4 may directly induce brain endothelial cell dysfunction via signaling (Nishitsuji et al., 2011), or indirectly through peripheral and central processes (Bell et al., 2012; Casey et al., 2015; Halliday et al., 2015). The interaction among the AD hits is equally as complex for two AD hits, which is amplified by the addition of a third. ApoE4 modulates A β levels, A β -dependent signaling, and the response to peripheral inflammation. Our ongoing studies are focused on delineating the potential CNS- and peripherally-relevant changes that may underlie these effects.

Through collective analysis of our data, we hypothesize that LPS-induced cerebrovascular and cognitive damage in E4FAD+ mice in response to repeated LPS challenge is mediated by complex processes within the central nervous system and the plasma in the paradigm utilized (i.e., LPS treatment from 4 to 6 months of age). In the central nervous system, the combination of *APOE4*- and A β -modulated processes (described earlier) converge, to predispose brain endothelial cells of the cerebrovasculature to damage. In the periphery, *APOE4* modulates the inflammatory response to LPS, resulting in a detrimental peripheral cytokine/chemokine profile that is characterized by higher detrimental and lower protective factors for brain endothelial cell function. The collective result is brain endothelial cell disruption, cerebrovascular leakiness, and cognitive impairment only in E4FAD+ mice. An important future direction is to determine whether E3FAD+ mice or E4FAD- mice are the next group to exhibit cerebrovasculature and cognitive impairments after longer LPS treatment.

In summary, peripheral inflammation interacts with *APOE4* and A β to induce and accelerate cerebrovascular and cognitive deficits. Thus, cerebrovascular dysfunction is a key mechanistic process linking AD hits to pathology.

Summary

Peripheral inflammation interacts with *APOE4* and A β to induce cerebrovascular and cognitive deficits.

Declaration of Conflicting Interests

The authors declared no potential conflicts of interest with respect to the research, authorship, and/or publication of this article.

Funding

The authors disclosed receipt of the following financial support for the research, authorship and/or publication of this article: Institutional funding from University of Illinois at Chicago College of Medicine.

Notes

1. For all representative mosaic images the following was conducted using the Zeiss Axio Imager M1 software and a motorized stage at 20 \times magnification: the boundaries of each individual brain section were set that included the hippocampus

and cortex using the mosaic function, sequential images were obtained that encompassed the entire area of the tissue boundary (between ~50 and 150 images per section), and all the individual images were then stitched together to produce a single composite image.

2. As apoE levels were assessed in EFAD+ and EFAD- mice, a three-way ANOVA *F* test was conducted.

References

- Alexandrakis, M. G., Goulidaki, N., Pappa, C. A., Boula, A., Psarakis, F., Neonakis, I., & Tsirakis, G. (2015). Interleukin-10 induces both plasma cell proliferation and angiogenesis in multiple myeloma. *Pathol Oncol Res*, *21*, 929–934.
- Ambrose, C. T. (2016). The role of capillaries in the lesser ailments of old age and in Alzheimer's disease and vascular Dementia: The potential of pro-therapeutic angiogenesis. *J Alzheimers Dis*, *54*, 31–43.
- Aslam, M., Ahmad, N., Srivastava, R., & Hemmer, B. (2012). TNF-alpha induced NFkappaB signaling and p65 (RelA) overexpression repress Cldn5 promoter in mouse brain endothelial cells. *Cytokine*, *57*, 269–275.
- Bell, R. D., Winkler, E. A., Singh, I., Sagare, A. P., Deane, R., Wu, Z., Holtzman, D. M., Betsholtz, C., Armulik, A., Sallstrom, J., Berk, B. C., & Zlokovic, B. V. (2012). Apolipoprotein E controls cerebrovascular integrity via cyclophilin A. *Nature*, *485*, 512–516.
- Bertram, L., & Tanzi, R. E. (2004). Alzheimer's disease: One disorder, too many genes? *Hum Mol Genet*, *13*(Suppl 1): R135–R141.
- Biron, K. E., Dickstein, D. L., Gopaul, R., & Jefferies, W. A. (2011). Amyloid triggers extensive cerebral angiogenesis causing blood brain barrier permeability and hypervascularity in Alzheimer's disease. *PLoS One*, *6*, e23789.
- Boscolo, E., Folin, M., Nico, B., Grandi, C., Mangieri, D., Longo, V., Scienza, R., Zampieri, P., Conconi, M. T., Parnigotto, P. P., Ribatti, D. (2007). Beta amyloid angiogenic activity in vitro and in vivo. *Int J Mol Med*, *19*, 581–587.
- Bouras, C., Kovari, E., Herrmann, F. R., Rivara, C. B., Bailey, T. L., von Gunten, A., Hof, P. R., & Giannakopoulos, P. (2006). Stereologic analysis of microvascular morphology in the elderly: Alzheimer disease pathology and cognitive status. *J Neuropathol Exp Neurol*, *65*, 235–244.
- Brugg, B., Dubreuil, Y. L., Huber, G., Wollman, E. E., Delhaye-Bouchaud, N. & Mariani, J. (1995). Inflammatory processes induce beta-amyloid precursor protein changes in mouse brain. *Proc Natl Acad Sci U S A*, *92*, 3032–3035.
- Bush, A. I., Martins, R. N., Rumble, B., Moir, R., Fuller, S., Milward, E., Currie, J., Ames, D., Weidemann, A., & Fischer, P. (1990). The amyloid precursor protein of Alzheimer's disease is released by human platelets. *J Biol Chem*, *265*, 15977–15983.
- Cameron, D. J., Galvin, C., Alkam, T., Sidhu, H., Ellison, J., Luna, S., & Ethell, D. W. (2012). Alzheimer's-related peptide amyloid-beta plays a conserved role in angiogenesis. *PLoS One*, *7*, e39598.
- Candeias, E., Duarte, A. I., Carvalho, C., Correia, S. C., Cardoso, S., Santos, R. X., Placido, A. I., Perry, G., & Moreira, P. I. (2012). The impairment of insulin signaling in Alzheimer's disease. *IUBMB Life*, *64*, 951–957.
- Casey, C. S., Atagi, Y., Yamazaki, Y., Shinohara, M., Tachibana, M., Fu, Y., Bu, G., & Kanekiyo, T. (2015). Apolipoprotein E

- inhibits cerebrovascular pericyte mobility through a RhoA-mediated pathway. *J Biol Chem*, 290, 14208–14217.
- Cates, A. M., Holden, V. I., Myers, E. M., Smith, C. K., Kaplan, M. J. & Kahlenberg, J. M. (2015). Interleukin 10 hampers endothelial cell differentiation and enhances the effects of interferon alpha on lupus endothelial cell progenitors. *Rheumatology (Oxford)*, 54, 1114–1123.
- Chen, J., Buchanan, J. B., Sparkman, N. L., Godbout, J. P., Freund, G. G. & Johnson, R. W. (2008). Neuroinflammation and disruption in working memory in aged mice after acute stimulation of the peripheral innate immune system. *Brain Behav Immun*, 22, 301–311.
- Christensen, D. Z., Bayer, T. A., & Wirths, O. (2009). Formic acid is essential for immunohistochemical detection of aggregated intraneuronal Aβ peptides in mouse models of Alzheimer's disease. *Brain Res*, 1301, 116–125.
- Corder, E. H., Saunders, A. M., Strittmatter, W. J., Schmechel, D. E., Gaskell, P. C., Small, G. W., Roses, A. D., Haines, J. L., & Pericak-Vance, M. A. (1993). Gene dose of apolipoprotein E type 4 allele and the risk of Alzheimer's disease in late onset families. *Science*, 261, 921–923.
- Cummings, B. J., Mason, A. J., Kim, R. C., Sheu, P. C., & Anderson, A. J. (2002). Optimization of techniques for the maximal detection and quantification of Alzheimer's-related neuropathology with digital imaging. *Neurobiol Aging*, 23, 161–170.
- Cunningham, C., Campion, S., Lunnon, K., Murray, C. L., Woods, J. F., Deacon, R. M., Rawlins, J. N., & Perry, V. H. (2009). Systemic inflammation induces acute behavioral and cognitive changes and accelerates neurodegenerative disease. *Biol Psychiatry*, 65, 304–312.
- Dace, D. S., Khan, A. A., Kelly, J., & Apte, R. S. (2008). Interleukin-10 promotes pathological angiogenesis by regulating macrophage response to hypoxia during development. *PLoS One*, 3, e3381.
- de Hoon, M. J., Imoto, S., Nolan, J., & Miyano, S. (2004). Open source clustering software. *Bioinformatics*, 20, 1453–1454.
- de la Torre, J. C. (2010). Vascular risk factor detection and control may prevent Alzheimer's disease. *Ageing Res Rev*, 9, 218–225.
- Dickstein, D. L., Biron, K. E., Ujiie, M., Pfeifer, C. G., Jeffries, A. R. & Jeffries, W. A. (2006). Aβ peptide immunization restores blood-brain barrier integrity in Alzheimer disease. *FASEB J*, 20, 426–433.
- Donnini, S., Solito, R., Cetti, E., Corti, F., Giachetti, A., Carra, S., Beltrame, M., Cotelli, F., & Ziche, M. (2010). Aβ peptides accelerate the senescence of endothelial cells in vitro and in vivo, impairing angiogenesis. *FASEB J*, 24, 2385–2395.
- Duncan, B. B., Schmidt, M. I., Pankow, J. S., Ballantyne, C. M., Couper, D., Vigo, A., Hoogeveen, R., Folsom, A. R., Heiss, G., & Atherosclerosis Risk in Communities, S. (2003). Low-grade systemic inflammation and the development of type 2 diabetes: The atherosclerosis risk in communities study. *Diabetes*, 52, 1799–1805.
- Duperray, A., Barbe, D., Raguenez, G., Weksler, B. B., Romero, I. A., Couraud, P. O., Perron, H., & Marche, P. N. (2015). Inflammatory response of endothelial cells to a human endogenous retrovirus associated with multiple sclerosis is mediated by TLR4. *Int Immunol*, 27, 545–553.
- Erickson, M. A., Hartvigson, P. E., Morofuji, Y., Owen, J. B., Butterfield, D. A. & Banks, W. A. (2012). Lipopolysaccharide impairs amyloid β efflux from brain: Altered vascular sequestration, cerebrospinal fluid reabsorption, peripheral clearance and transporter function at the blood-brain barrier. *J Neuroinflammation*, 9, 150.
- Farkas, E., & Luiten, P. G. (2001). Cerebral microvascular pathology in aging and Alzheimer's disease. *Prog Neurobiol*, 64, 575–611.
- Farrer, L. A., Cupples, L. A., Haines, J. L., Hyman, B., Kukull, W. A., Mayeux, R., Myers, R. H., Pericak-Vance, M. A., Risch, N., & van Duijn, C. M. (1997). Effects of age, sex, and ethnicity on the association between apolipoprotein E genotype and Alzheimer disease. A meta-analysis. APOE and Alzheimer Disease Meta Analysis Consortium. *JAMA*, 278, 1349–1356.
- Gale, S. C., Gao, L., Mikacenic, C., Coyle, S. M., Rafaels, N., Murray Dudenkov, T., Madenspacher, J. H., Draper, D. W., Ge, W., Aloor, J. J., Azzam, K. M., Lai, L., Blackshear, P. J., Calvano, S. E., Barnes, K. C., Lowry, S. F., Corbett, S., Wurfel, M. M., & Fessler, M. B. (2014). APOε4 is associated with enhanced in vivo innate immune responses in human subjects. *J Allergy Clin Immunol*, 134, 127–134.
- Genin, E., et al. (2011). APOE and Alzheimer disease: a major gene with semi-dominant inheritance. *Mol Psychiatry*, 16, 903–907.
- Giannoni, P., Arango-Lievano, M., Neves, I. D., Rousset, M. C., Baranger, K., Rivera, S., Jeanneteau, F., Claeysen, S., & Marchi, N. (2016). Cerebrovascular pathology during the progression of experimental Alzheimer's disease. *Neurobiol Dis*, 88, 107–117.
- Haan, M. N., Shemanski, L., Jagust, W. J., Manolio, T. A., & Kuller, L. (1999). The role of APOE ε4 in modulating effects of other risk factors for cognitive decline in elderly persons. *JAMA*, 282, 40–46.
- Halliday, M. R., Rege, S. V., Ma, Q., Zhao, Z., Miller, C. A., Winkler, E. A., & Zlokovic, B. V. (2015). Accelerated pericyte degeneration and blood-brain barrier breakdown in apolipoprotein E4 carriers with Alzheimer's disease. *J Cereb Blood Flow Metab*, 36, 216–227.
- Hansson, G. K., Robertson, A. K., & Soderberg-Naucler, C. (2006). Inflammation and atherosclerosis. *Annu Rev Pathol*, 1, 297–329.
- Hashimura, T., Kimura, T., & Miyakawa, T. (1991). Morphological changes of blood vessels in the brain with Alzheimer's disease. *Jpn J Psychiatry Neurol*, 45, 661–665.
- Haus-Wegrzyniak, B., Dobrzanski, P., Stoehr, J. D., & Wenk, G. L. (1998). Chronic neuroinflammation in rats reproduces components of the neurobiology of Alzheimer's disease. *Brain Res*, 780, 294–303.
- Henry-Feugeas, M. C. (2008). Alzheimer's disease in late-life dementia: A minor toxic consequence of devastating cerebrovascular dysfunction. *Med Hypotheses*, 70, 866–875.
- Iadecola, C. (2004). Neurovascular regulation in the normal brain and in Alzheimer's disease. *Nat Rev Neurosci*, 5, 347–360.
- Irie, F., Fitzpatrick, A. L., Lopez, O. L., Kuller, L. H., Peila, R., Newman, A. B., & Launer, L. J. (2008). Enhanced risk for Alzheimer disease in persons with type 2 diabetes and APOE ε4: The Cardiovascular Health Study Cognition Study. *Arch Neurol*, 65, 89–93.
- Jaeger, L. B., Dohgu, S., Sultana, R., Lynch, J. L., Owen, J. B., Erickson, M. A., Shah, G. N., Price, T. O., Fleegal-Demotta, M. A., Butterfield, D. A., & Banks, W. A. (2009). Lipopolysaccharide alters the blood-brain barrier transport of amyloid β protein: A mechanism for inflammation in the progression of Alzheimer's disease. *Brain Behav Immun*, 23, 507–517.

- Jantarotnotai, N., Ryu, J. K., Schwab, C., McGeer, P. L., & McLarnon, J. G. (2011). Comparison of vascular perturbations in an abeta-injected animal model and in AD brain. *Int J Alzheimers Dis*, 2011, 918280.
- Joshi, Y. B., & Pratico, D. (2014). The 5-lipoxygenase pathway: oxidative and inflammatory contributions to the Alzheimer's disease phenotype. *Front Cell Neurosci*, 8, 436.
- Kahn, M. S., Kranjac, D., Alonzo, C. A., Haase, J. H., Cedillos, R. O., McLinden, K. A., Boehm, G. W., & Chumley, M. J. (2012). Prolonged elevation in hippocampal Abeta and cognitive deficits following repeated endotoxin exposure in the mouse. *Behav Brain Res*, 229, 176–184.
- Kawabe, J., Koda, M., Hashimoto, M., Fujiyoshi, T., Furuya, T., Endo, T., Okawa, A., & Yamazaki, M. (2011). Neuroprotective effects of granulocyte colony-stimulating factor and relationship to promotion of angiogenesis after spinal cord injury in rats: Laboratory investigation. *J Neurosurg Spine*, 15, 414–421.
- Kitaguchi, H., Ihara, M., Saiki, H., Takahashi, R., & Tomimoto, H. (2007). Capillary beds are decreased in Alzheimer's disease, but not in Binswanger's disease. *Neurosci Lett*, 417, 128–131.
- Kitamoto, T., Ogomori, K., Tateishi, J., & Prusiner, S. B. (1987). Formic acid pretreatment enhances immunostaining of cerebral and systemic amyloids. *Lab Invest*, 57, 230–236.
- Kohno, T., Mizukami, H., Suzuki, M., Saga, Y., Takei, Y., Shimpo, M., Matsushita, T., Okada, T., Hanazono, Y., Kume, A., Sato, I., & Ozawa, K. (2003). Interleukin-10-mediated inhibition of angiogenesis and tumor growth in mice bearing VEGF-producing ovarian cancer. *Cancer Res*, 63, 5091–5094.
- Koster, K. P., Thomas, R., Morris, A. W., & Tai, L. M. (2016). Epidermal growth factor prevents oligomeric amyloid-beta induced angiogenesis deficits in vitro. *J Cereb Blood Flow Metab*, 36, 1865–1871.
- Lee, J. W., Lee, Y. K., Yuk, D. Y., Choi, D. Y., Ban, S. B., Oh, K. W., & Hong, J. T. (2008). Neuro-inflammation induced by lipopolysaccharide causes cognitive impairment through enhancement of beta-amyloid generation. *J Neuroinflammation*, 5, 37.
- Lee, S. T., Chu, K., Park, J. E., Jung, K. H., Jeon, D., Lim, J. Y., Lee, S. K., Kim, M., & Roh, J. K. (2012). Erythropoietin improves memory function with reducing endothelial dysfunction and amyloid-beta burden in Alzheimer's disease models. *J Neurochem*, 120, 115–124.
- Leoni, V. (2011). The effect of apolipoprotein E (ApoE) genotype on biomarkers of amyloidogenesis, tau pathology and neurodegeneration in Alzheimer's disease. *Clin Chem Lab Med*, 49, 375–383.
- Liu, G. T., Huang, Y. L., Tzeng, H. E., Tsai, C. H., Wang, S. W. & Tang, C. H. (2015a). CCL5 promotes vascular endothelial growth factor expression and induces angiogenesis by down-regulating miR-199a in human chondrosarcoma cells. *Cancer Lett*, 357, 476–487.
- Liu, J., Duan, Y., Cheng, X., Chen, X., Xie, W., Long, H., Lin, Z., & Zhu, B. (2011). IL-17 is associated with poor prognosis and promotes angiogenesis via stimulating VEGF production of cancer cells in colorectal carcinoma. *Biochem Biophys Res Commun*, 407, 348–354.
- Liu, X. Y., Gonzalez-Toledo, M. E., Fagan, A., Duan, W. M., Liu, Y., Zhang, S., Li, B., Piao, C. S., Nelson, L., & Zhao, L. R. (2015b). Stem cell factor and granulocyte colony-stimulating factor exhibit therapeutic effects in a mouse model of CADASIL. *Neurobiol Dis*, 73, 189–203.
- Lopez-Ramirez, M. A., Male, D. K., Wang, C., Sharrack, B., Wu, D. & Romero, I. A. (2013). Cytokine-induced changes in the gene expression profile of a human cerebral microvascular endothelial cell-line, hCMEC/D3. *Fluids Barriers CNS*, 10, 27.
- Love, S., & Miners, J. S. (2016). Cerebrovascular disease in ageing and Alzheimer's disease. *Acta Neuropathol*, 131, 645–658.
- Marsland, A. L., Gianaros, P. J., Kuan, D. C., Sheu, L. K., Krajina, K. & Manuck, S. B. (2015). Brain morphology links systemic inflammation to cognitive function in midlife adults. *Brain Behav Immun*, 48, 195–204.
- Matsuo, Y., Raimondo, M., Woodward, T. A., Wallace, M. B., Gill, K. R., Tong, Z., Burdick, M. D., Yang, Z., Strieter, R. M., Hoffman, R. M., & Guha, S. (2009). CXC-chemokine/CXCR2 biological axis promotes angiogenesis in vitro and in vivo in pancreatic cancer. *Int J Cancer*, 125, 1027–1037.
- Matsuzaki, T., Sasaki, K., Tanizaki, Y., Hata, J., Fujimi, K., Matsui, Y., Sekita, A., Suzuki, S. O., Kanba, S., Kiyohara, Y., & Iwaki, T. (2010). Insulin resistance is associated with the pathology of Alzheimer disease: The Hisayama study. *Neurology*, 75, 764–770.
- Meredith, M. E., Salameh, T. S., & Banks, W. A. (2015). Intranasal delivery of proteins and peptides in the treatment of neurodegenerative diseases. *AAPS J*, 17, 780–787.
- Meyer, E. P., Ulmann-Schuler, A., Staufenbiel, M., & Krucker, T. (2008). Altered morphology and 3D architecture of brain vasculature in a mouse model for Alzheimer's disease. *Proc Natl Acad Sci U S A*, 105, 3587–3592.
- Michaud, J. P., Halle, M., Lampron, A., Theriault, P., Prefontaine, P., Filali, M., Tribout-Jover, P., Lanteigne, A. M., Jodoin, R., Cluff, C., Brichard, V., Palmantier, R., Pilorget, A., Larocque, D., & Rivest, S. (2013). Toll-like receptor 4 stimulation with the detoxified ligand monophosphoryl lipid A improves Alzheimer's disease-related pathology. *Proc Natl Acad Sci U S A*, 110, 1941–1946.
- Miyakawa, T. (2010). Vascular pathology in Alzheimer's disease. *Psychogeriatrics*, 10, 39–44.
- Miyake, M., Goodison, S., Urquidi, V., Gomes Giacoia, E., & Rosser, C. J. (2013). Expression of CXCL1 in human endothelial cells induces angiogenesis through the CXCR2 receptor and the ERK1/2 and EGF pathways. *Lab Invest*, 93, 768–778.
- Nishitsuji, K., Hosono, T., Nakamura, T., Bu, G., & Michikawa, M. (2011). Apolipoprotein E regulates the integrity of tight junctions in an isoform-dependent manner in an in vitro blood-brain barrier model. *J Biol Chem*, 286, 17536–17542.
- Paris, D., Patel, N., DelleDonne, A., Quadros, A., Smeed, R. & Mullan, M. (2004). Impaired angiogenesis in a transgenic mouse model of cerebral amyloidosis. *Neurosci Lett*, 366, 80–85.
- Paul, J., Strickland, S., & Melchor, J. P. (2007). Fibrin deposition accelerates neurovascular damage and neuroinflammation in mouse models of Alzheimer's disease. *J Exp Med*, 204, 1999–2008.
- Pickens, S. R., Volin, M. V., Mandelin, A. M. 2nd, Kolls, J. K., Pope, R. M. & Shahrara, S. (2010). IL-17 contributes to angiogenesis in rheumatoid arthritis. *J Immunol*, 184, 3233–3241.
- Pugh, C. R., Kumagawa, K., Fleshner, M., Watkins, L. R., Maier, S. F. & Rudy, J. W. (1998). Selective effects of peripheral lipopolysaccharide administration on contextual and auditory-cue fear conditioning. *Brain Behav Immun*, 12, 212–229.
- Qin, L. H., Huang, W., Mo, X. A., Chen, Y. L., & Wu, X. H. (2015). LPS induces occludin dysregulation in cerebral

- microvascular endothelial cells via MAPK signaling and augmenting MMP-2 levels. *Oxid Med Cell Longev*, 2015, 120641.
- Core Team, R (2014). *R: A language and environment for statistical computing*. Vienna, Austria: R Foundation for Statistical Computing.
- Roberts, T. K., Eugenin, E. A., Lopez, L., Romero, I. A., Weksler, B. B., Couraud, P. O., & Berman, J. W. (2012). CCL2 disrupts the adherens junction: Implications for neuroinflammation. *Lab Invest*, 92, 1213–1233.
- Saldanha, A. J. (2004). Java Treeview—extensible visualization of microarray data. *Bioinformatics*, 20, 3246–3248.
- Savoia, C., & Schiffrin, E. L. (2006). Inflammation in hypertension. *Curr Opin Nephrol Hypertens*, 15, 152–158.
- Scalia, R., Appel, J. Z. 3rd, & Lefer, A. M. (1998). Leukocyte-endothelium interaction during the early stages of hypercholesterolemia in the rabbit: Role of P-selectin, ICAM-1, and VCAM-1. *Arterioscler Thromb Vasc Biol*, 18, 1093–1100.
- Shaw, K. N., Commins, S., & O'Mara, S. M. (2001). Lipopolysaccharide causes deficits in spatial learning in the watermaze but not in BDNF expression in the rat dentate gyrus. *Behav Brain Res*, 124, 47–54.
- Shinohara, M., Murray, M. E., Frank, R. D., Shinohara, M., DeTure, M., Yamazaki, Y., Tachibana, M., Atagi, Y., Davis, M. D., Liu, C. C., Zhao, N., Painter, M. M., Petersen, R. C., Fryer, J. D., Crook, J. E., Dickson, D. W., Bu, G., & Kanekiyo, T. (2016). Impact of sex and APOE4 on cerebral amyloid angiopathy in Alzheimer's disease. *Acta Neuropathol*, 132, 225–234.
- Sparkman, N. L., Kohman, R. A., Garcia, A. K., & Boehm, G. W. (2005). Peripheral lipopolysaccharide administration impairs two-way active avoidance conditioning in C57BL/6J mice. *Physiol Behav*, 85, 278–288.
- Stanimirovic, D. B., & Friedman, A. (2012). Pathophysiology of the neurovascular unit: Disease cause or consequence? *J Cereb Blood Flow Metab*, 32, 1207–1221.
- Strasly, M., Cavallo, F., Geuna, M., Mitola, S., Colombo, M. P., Forni, G., & Bussolino, F. (2001). IL-12 inhibition of endothelial cell functions and angiogenesis depends on lymphocyte-endothelial cell cross-talk. *J Immunol*, 166, 3890–3899.
- Suffee, N., Hlawaty, H., Meddahi-Pelle, A., Maillard, L., Louedec, L., Haddad, O., Martin, L., Laguillier, C., Richard, B., Oudar, O., Letourneur, D., Chamaux, N., & Sutton, A. (2012). RANTES/CCL5-induced pro-angiogenic effects depend on CCR1, CCR5 and glycosaminoglycans. *Angiogenesis*, 15, 727–744.
- Tai, L. M., Mehra, S., Shete, V., Estus, S., Rebeck, G. W., Bu, G., & Ladu, M. J. (2014). Soluble apoE/Abeta complex: Mechanism and therapeutic target for APOE4-induced AD risk. *Mol Neurodegener*, 9, 2.
- Tai, L. M., Thomas, R., Marottoli, F. M., Koster, K. P., Kanekiyo, T., Morris, A. W., & Bu, G. (2016). The role of APOE in cerebrovascular dysfunction. *Acta Neuropathol*, 131, 709–723.
- Tai, L. M., Balu, D., Avila-Munoz, E., Abdullah, L., Thomas, R., Collins, N., Valencia-Olvera, A. C., & LaDu, M. J. (2017). EFAD transgenic mice as a human APOE relevant preclinical model of Alzheimer's disease. *J Lipid Res*. Advance online publication. doi:10.1194/jlr.R076315.
- Thomas, R., Zuchowska, P., Morris, A. W., Marottoli, F. M., Sunny, S., Deaton, R., Gann, P. H., & Tai, L. M. (2016). Epidermal growth factor prevents APOE4 and amyloid-beta-induced cognitive and cerebrovascular deficits in female mice. *Acta Neuropathol Commun*, 4, 111.
- Thomson, L. M., & Sutherland, R. J. (2005). Systemic administration of lipopolysaccharide and interleukin-1beta have different effects on memory consolidation. *Brain Res Bull*, 67, 24–29.
- Tura, O., Crawford, J., Barclay, G. R., Samuel, K., Hadoke, P. W., Roddie, H., Davies, J., & Turner, M. L. (2010). Granulocyte colony-stimulating factor (G-CSF) depresses angiogenesis in vivo and in vitro: implications for sourcing cells for vascular regeneration therapy. *J Thromb Haemost*, 8, 1614–1623.
- Ujje, M., Dickstein, D. L., Carlow, D. A., & Jefferies, W. A. (2003). Blood-brain barrier permeability precedes senile plaque formation in an Alzheimer disease model. *Microcirculation*, 10, 463–470.
- van de Haar, H. J., Burgmans, S., Hofman, P. A., Verhey, F. R., Jansen, J. F., & Backes, W. H. (2015). Blood-brain barrier impairment in dementia: Current and future in vivo assessments. *Neurosci Biobehav Rev*, 49C, 71–81.
- Vaure, C., & Liu, Y. (2014). A comparative review of toll-like receptor 4 expression and functionality in different animal species. *Front Immunol*, 5, 316.
- Vinters, H. V. (1987). Cerebral amyloid angiopathy. *A critical review*. *Stroke*, 18, 311–324.
- Wang, D., Wang, H., Brown, J., Daikoku, T., Ning, W., Shi, Q., Richmond, A., Strieter, R., Dey, S. K., & DuBois, R. N. (2006). CXCL1 induced by prostaglandin E2 promotes angiogenesis in colorectal cancer. *J Exp Med*, 203, 941–951.
- Wang, S. W., Liu, S. C., Sun, H. L., Huang, T. Y., Chan, C. H., Yang, C. Y., Yeh, H. I., Huang, Y. L., Chou, W. Y., Lin, Y. M., & Tang, C. H. (2015). CCL5/CCR5 axis induces vascular endothelial growth factor-mediated tumor angiogenesis in human osteosarcoma microenvironment. *Carcinogenesis*, 36, 104–114.
- Wei, X., Xu, Y., Jin, Y., Feng, H., & Dong, S. (2017). Granulocyte colony-stimulating factor attenuates blood-brain barrier damage and improves cognitive function in spontaneously hypertensive rats. *CNS Neurol Disord Drug Targets*. Advance online publication. doi: 10.2174/1871527316666170207155730.
- Youmans, K. L., Tai, L. M., Nwabuisi-Heath, E., Jungbauer, L., Kanekiyo, T., Gan, M., Kim, J., Eimer, W. A., Estus, S., Rebeck, G. W., Weeber, E. J., Bu, G., Yu, C., & Ladu, M. J. (2012a). APOE4-specific changes in Abeta accumulation in a new transgenic mouse model of Alzheimer disease. *J Biol Chem*, 287, 41774–41786.
- Youmans, K. L., Tai, L. M., Kanekiyo, T., Stine, W. B. Jr., Michon, S. C., Nwabuisi-Heath, E., Manelli, A., Fu, Y., Riordan, S., Eimer, W. A., Binder, L., Bu, G., Yu, C., Hartley, D. M., & Ladu, M. J. (2012b). Intraneuronal Abeta detection in 5xFAD mice by a new Abeta-specific antibody. *Mol Neurodegener*, 7, 8.
- Zhou, Y., Yoshida, S., Kubo, Y., Kobayashi, Y., Nakama, T., Yamaguchi, M., Ishikawa, K., Nakao, S., Ikeda, Y., Ishibashi, T., & Sonoda, K. H. (2016). Interleukin-12 inhibits pathological neovascularization in mouse model of oxygen-induced retinopathy. *Sci Rep*, 6, 28140.
- Zlokovic, B. V. (2011). Neurovascular pathways to neurodegeneration in Alzheimer's disease and other disorders. *Nat Rev Neurosci*, 12, 723–738.